

1 **All about Nitrite: Exploring Nitrite Sources and Sinks in the Eastern Tropical North**  
2 **Pacific Oxygen Minimum Zone**

3

4 John C. Tracey<sup>1,2</sup>, Andrew R. Babbin<sup>3</sup>, Elizabeth Wallace<sup>1</sup>, Xin Sun<sup>1,4</sup>, Katherine L. DuRussel<sup>1,</sup>  
5 <sup>5</sup>, Claudia Frey<sup>1,6</sup>, Donald E. Martocello III<sup>3</sup>, Tyler Tamasi<sup>3</sup>, Sergey Oleynik<sup>1</sup>, and Bess B.  
6 Ward<sup>1</sup>

7

8 <sup>1</sup> Department of Geosciences, Princeton University, Guyot Hall, Princeton, NJ, USA 08544  
9 <sup>2</sup> Department of Biology and Paleo Environment, Lamont Doherty Earth Observatory, Columbia  
10 University, Palisades, NY, USA 10964  
11 <sup>3</sup> Department of Earth, Atmospheric and Planetary Sciences, Massachusetts Institute of  
12 Technology, Cambridge, MA, USA 02138  
13 <sup>4</sup> Department of Global Ecology, Carnegie Institution for Science, Stanford, CA, USA 94305  
14 <sup>5</sup> Department of Civil and Environmental Engineering, Northwestern University, Evanston, IL,  
15 USA 60208  
16 <sup>6</sup> Department of Environmental Sciences, University of Basel, Bernoullistrasse 30, 4056 Basel,  
17 Switzerland  
18

19 *Correspondence to:* John C. Tracey (jt16@~~alumni~~-princeton.edu)

20

21

22

23

24

25

26

27

28

29 **Abstract**

30 Oxygen minimum zones (OMZs), due to their large volumes of perennially deoxygenated  
31 waters, are critical regions for understanding how the interplay between anaerobic and aerobic  
32 nitrogen (N) cycling microbial pathways affects the marine N budget. Here we present a suite of  
33 measurements of the most significant OMZ N cycling rates, which all involve nitrite ( $\text{NO}_2^-$ ) as a  
34 product, reactant, or intermediate, in the Eastern Tropical North Pacific (ETNP) OMZ. These  
35 measurements and comparisons to data from previously published OMZ cruises present  
36 additional evidence that  $\text{NO}_3^-$  reduction is the predominant OMZ N flux, followed by  $\text{NO}_2^-$   
37 oxidation back to  $\text{NO}_3^-$ . The combined rates of both of these N recycling processes were  
38 observed to be much greater (up to nearly 200x) than the combined rates of the N loss processes  
39 of anammox and denitrification, especially in waters near the anoxic / oxic interface. We also  
40 show that  $\text{NO}_2^-$  oxidation can occur when  $\text{O}_2$  is maintained near 1 nM by a continuous purge  
41 system in functionally anoxic incubations,  $\text{NO}_2^-$  oxidation and  $\text{O}_2$  measurements that further  
42 strengthen the case for truly anaerobic  $\text{NO}_2^-$  oxidation. We also evaluate the possibility that  
43  $\text{NO}_2^-$  dismutation provides the oxidative power for anaerobic  $\text{NO}_2^-$  oxidation. ~~Although almost~~  
44 ~~all treatments returned little evidence for dismutation (as based on product inhibition, substrate~~  
45 ~~stimulation, and stoichiometric hypotheses), results from one treatment under conditions closest~~  
46 ~~to in situ  $\text{NO}_2^-$  values may support the occurrence of  $\text{NO}_2^-$  dismutation.~~ The partitioning of N  
47 loss between anammox and denitrification differed widely from stoichiometric predictions of at  
48 most 29% anammox; in fact, N loss rates at many depths were entirely due to~~consisted entirely~~  
49 ~~of~~ anammox. ~~Through investigating the magnitudes of  $\text{NO}_3^-$  reduction and  $\text{NO}_2^-$  oxidation,~~  
50 ~~testing for anaerobic  $\text{NO}_2^-$  oxidation, examining the possibility of  $\text{NO}_2^-$  dismutation, and further~~  
51 ~~documenting the balance of N loss processes,~~ Our these new  $\text{NO}_3^-$  reduction,  $\text{NO}_2^-$  oxidation,

52 dismutation, and N loss data shed light on many open questions in OMZ N cycling research,  
53 especially the possibility of truly anaerobic  $\text{NO}_2^-$  oxidation.

54

## 55 **1. Introduction**

56 Nitrogen (N) is essential for life because of its prominent role in DNA, RNA, and protein  
57 chemistry. As a result, N limits biological productivity in many marine environments. The  
58 dissimilatory biological N loss and recycling pathways are traditionally understood to be strictly  
59 separated by  $\text{O}_2$  tolerance. The N loss processes of denitrification, the stepwise reduction of  
60  $\text{NO}_3^-$  to  $\text{N}_2$ , and anaerobic ammonium oxidation (anammox), the oxidation of  $\text{NH}_4^+$  with  $\text{NO}_2^-$  to  
61 make  $\text{N}_2$ , require low  $\text{O}_2$  while the N recycling pathways of  $\text{NH}_4^+$  oxidation to  $\text{NO}_2^-$  and  $\text{NO}_2^-$   
62 oxidation to  $\text{NO}_3^-$  are viewed as obligately aerobic. Importantly,  $\text{NO}_2^-$  is a product, reactant, or  
63 intermediate in all these pathways. Therefore, developing an understanding of  $\text{NO}_2^-$  sources and  
64 sinks is essential for a complete understanding of marine N biogeochemistry.

65 Oxygen minimum zones (OMZs) and sediments are the two main marine environments  
66 where N loss occurs. There are three major OMZs, the Eastern Tropical North Pacific (ETNP),  
67 the Eastern Tropical South Pacific (ETSP), and the Arabian Sea, which occupy 0.1 - 1% of total  
68 ocean volume, depending on the  $\text{O}_2$  threshold used (Codispoti and Richards, 1976; Naqvi, 1987;  
69 Bange et al., 2000; Codispoti et al., 2005; Lam and Kuypers, 2011). Importantly, the OMZ water  
70 column is not completely deoxygenated from top to bottom; OMZs are characterized by an  
71 oxygenated surface, a depth interval of steeply declining  $\text{O}_2$  around the mixed layer depth, called  
72 the oxycline, an oxygen deficient zone (ODZ) spanning several hundred meters where  $\text{O}_2$   
73 declines below the detection limit of common shipboard CTD  $\text{O}_2$  sensors, and then a second,  
74 gradual, oxycline that transitions to oxygenated deep water. Despite OMZ regions' small size,

75 they are responsible for ~~320~~-540% of total marine N loss (DeVries et al., 2013), a magnitude  
76 significant for the global marine N budget. In this work, in order to answer several open  
77 questions about OMZs and marine N cycling, we conducted a suite of <sup>15</sup>N stable isotope  
78 measurements of the most important N cycling microbial pathways in OMZs. We report the N  
79 loss rates of anammox and denitrification, as well as the N recycling rates of NO<sub>3</sub><sup>-</sup> reduction,  
80 NO<sub>2</sub><sup>-</sup> oxidation, and NH<sub>4</sub><sup>+</sup> oxidation, all of which involve NO<sub>2</sub><sup>-</sup>.

81 A distinctive feature of OMZs is a secondary nitrite maximum (SNM) (Codispoti et al.,  
82 2001; Brandhorst, 1959; Codispoti and Packard, 1980). The highest nitrite concentrations within  
83 the SNM can reach 10 μM, much higher than the peak values found in the primary nitrite  
84 maximum at the base of the photic zone, which average ~100 nM globally (Lomas and  
85 Lipschultz, 2006). Several recent works have shown or argued that the SNM's NO<sub>2</sub><sup>-</sup> is supplied  
86 via high rates of the first step of denitrification, NO<sub>3</sub><sup>-</sup> reduction to NO<sub>2</sub><sup>-</sup> (Lam et al., 2009; Lam  
87 and Kuypers, 2011; Kalvelage et al., 2013; Babbin et al., 2017, 2020). NO<sub>3</sub><sup>-</sup> reduction has been  
88 proposed (Anderson et al., 1982) to be one-half of a rapid loop where NO<sub>3</sub><sup>-</sup> and NO<sub>2</sub><sup>-</sup> are  
89 recycled through simultaneously occurring NO<sub>3</sub><sup>-</sup> reduction and NO<sub>2</sub><sup>-</sup> oxidation. This loop has  
90 been supported through experimental measurements of both rates (Babbin et al., 2017, 2020;  
91 Kalvelage et al., 2013; Lipschultz et al., 1990). In this view, elevated NO<sub>3</sub><sup>-</sup> reduction also  
92 generates NH<sub>4</sub><sup>+</sup>, via organic matter (OM) remineralization, which enhances anammox at the  
93 expense of denitrification in oxycline and upper ODZ waters (Babbin et al., 2020). In this study,  
94 we conducted tests to further document this rapid loop's existence and role in enhancing  
95 anammox.

96 Recent measurements of NO<sub>2</sub><sup>-</sup> oxidation have returned significant rates from both the  
97 oxycline and the ODZ, findings that challenge the paradigm that NO<sub>2</sub><sup>-</sup> oxidation is an obligately

98 aerobic process. Evidence for high, widespread  $\text{NO}_2^-$  oxidation rates in low  $\text{O}_2$  waters has  
99 accumulated from direct rate measurements via  $^{15}\text{N}$  tracers (Füssel et al., 2011; Lipschultz et al.,  
100 1990; Peng et al., 2015, 2016; Ward et al., 1989; Kalvelage et al., 2013; Tsementzi et al., 2016;  
101 Sun et al., 2017, 2021a; Babbín et al., 2017, 2020), models (Buchwald et al., 2015), and  $^{15}\text{N}$   
102 natural abundance measurements (Casciotti et al., 2013). Many explanations have been  
103 proposed including microaerophilic nitrite oxidizing bacteria (NOB) adapted to low but non-zero  
104  $\text{O}_2$  conditions (Penn et al., 2016; Bristow et al., 2016; Tsementzi et al., 2016; Bristow et al.,  
105 2017) where the  $\text{O}_2$  for these NOB is transiently supplied to previously deoxygenated waters by  
106 ~~(+) (1)~~ vertical or horizontal mixing of the ocean surface or nearby oxic water (Casciotti et al.,  
107 2013; Tiano et al., 2014; Bristow et al., 2016; Ulloa et al., 2012), even into the anoxic ODZ  
108 (Margolskee et al., 2019; Monreal et al., 2022), or (2) a ~~or (2) a~~ cryptic  $\text{O}_2$  cycle where low-light  
109 adapted phototrophs produce  $\text{O}_2$  that is consumed by NOB (García-Robledo et al., 2017;  
110 Fuchsman et al., 2019).

111 Despite the power of~~While~~ these explanations, they do not preclude the possibility of  
112 widespread NOB capable of truly anaerobic ~~could account for oxycline and ODZ top~~  
113 ~~observations, they cannot account for rigorously  $\text{O}_2$  contamination controlled observations of~~  
114  $\text{NO}_2^-$  oxidation, especially in waters from the deep, dark, and deoxygenated ODZ core. ~~(Babbín~~  
115 ~~et al., 2020; Sun et al., 2021).~~ This possibility is ~~ese ODZ core results are~~ bolstered by  
116 sequencing data that show the presence of an NOB metagenome assembled genome (MAG) with  
117 a preference for ~~exclusive to~~ the deoxygenated ODZ core in the ETSP (Sun et al., 2019) and ~~and~~  
118 ODZ core kinetics experiments where  $\text{O}_2$  concentrations above  $5 \mu\text{M}$  ~~inhibits~~  $\text{NO}_2^-$  oxidation  
119 (Sun et al., 2021a). ~~Here we build on~~ past these stable isotope experimental results by  
120 performing additional depth profile experiments with purged waters from the ODZ and  $\text{O}_2$

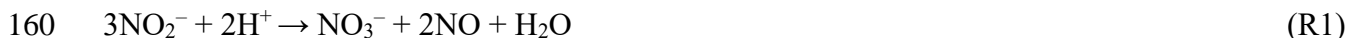
121 manipulation <sup>15</sup>N tracer experiments across a gradient of O<sub>2</sub> concentrations from 1 nM to 10  
122 μM. Our O<sub>2</sub> manipulation experiments, unlike previous studies, were conducted in vessels that  
123 were continuously purged throughout each incubation with a precisely calibrated mixture of N<sub>2</sub>,  
124 O<sub>2</sub>, and CO<sub>2</sub>. This experimental design allowed us to continuously maintain low O<sub>2</sub> conditions.  
125 In addition, our oxygen concentrations in these assays were verified via a LUMOS sensor, a  
126 sensor class with a detection limit of 0.5 nM O<sub>2</sub> (Lehner et al., 2015). Together, these method  
127 improvements convincingly show that the O<sub>2</sub> contamination observed to occur in Niskin  
128 sampling (Garcia-Robledo et al., 2016, 2021) is removed and that vanishingly low O<sub>2</sub> is  
129 maintained throughout the experiment.

130 ~~, including functionally anoxic (< 3 nM) O<sub>2</sub> concentrations where O<sub>2</sub> cannot play a~~  
131 ~~significant biological or biogeochemical role (Berg et al., 2022).~~

132 Anaerobic NO<sub>2</sub><sup>-</sup> oxidation would require an alternative oxidant other than O<sub>2</sub>. Many  
133 candidates have been proposed (Sun et al., 2023) for this oxidant including IO<sub>3</sub><sup>-</sup> (Babbin et al.,  
134 2017), Mn<sup>4+</sup>, Fe<sup>3+</sup> (Sun et al., 2021a), the anammox core metabolism (Sun et al., 2021a), the  
135 observed reversibility of the nitrite oxidoreductase enzyme (Wunderlich et al., 2013; Kemeny et  
136 al., 2016; Koch et al., 2015; Buchwald and Wankel, 2022), and NO<sub>2</sub><sup>-</sup> dismutation (Babbin et al.,  
137 2020; Füssel et al., 2011; Sun et al., 2021a). Due to multiple considerations such as very low  
138 IO<sub>3</sub><sup>-</sup> in the ODZ core (Moriyasu et al., 2020), low favorability of Mn<sup>4+</sup> or Fe<sup>3+</sup> mediated NO<sub>2</sub><sup>-</sup>  
139 oxidation at marine pH values (Luther, 2010), low anammox rates that do not explain the  
140 observed stoichiometry of NO<sub>2</sub><sup>-</sup> oxidation to anammox (Kalvelage et al., 2013; Babbin et al.,  
141 2020; Sun et al., 2021a), and ~~uncertainty if~~ the inability of the enzyme hypothesis ~~to~~ account  
142 for structural and phylogenetic differences in the NXR of the four NOB genera (Buchwald and

143 Wankel, 2022; Sun et al., 2019), we conducted experiments to test the remaining most plausible  
144 hypothesis: NO<sub>2</sub><sup>-</sup> dismutation.

145 NO<sub>2</sub><sup>-</sup> dismutation (Eq. (R4)) is energetically favorable (Strohm et al., 2007; Van de  
146 Leemput et al., 2011) although it has not been detected in nature. The reaction is proposed to  
147 occur in three steps (Eq. (R1-3)) (Babbin et al., 2020) and [DNA sequences that encode](#) possible  
148 enzymes for steps [two2](#) and [three3](#) (Eqs. (R2, R3)) have been found in ODZ core metagenomic  
149 reads and ~~metagenome assembled genomes (MAGs)~~ (Padilla et al., 2016; Babbin et al., 2020).  
150 While these sequences were not classified as NOB, they do indicate that parts of the pathway  
151 could occur in OMZs. If discovered in OMZs, NO<sub>2</sub><sup>-</sup> dismutation would be another N loss  
152 pathway, albeit one indistinguishable from denitrification since the <sup>15</sup>N atoms in <sup>30</sup>N<sub>2</sub> come from  
153 <sup>15</sup>NO<sub>2</sub><sup>-</sup> in both pathways. Here we evaluate the hypothesis that NO<sub>2</sub><sup>-</sup> dismutation is a significant  
154 mechanism for NO<sub>2</sub><sup>-</sup> oxidation under low O<sub>2</sub>, by searching for product inhibition, the inhibition  
155 of both NO<sub>2</sub><sup>-</sup> oxidation and <sup>30</sup>N<sub>2</sub> production (i.e. denitrification) in response to addition of NO<sub>3</sub><sup>-</sup>,  
156 substrate stimulation (increases in both <sup>30</sup>N<sub>2</sub> production and NO<sub>2</sub><sup>-</sup> oxidation in response to  
157 addition of <sup>15</sup>NO<sub>2</sub><sup>-</sup>), and by comparing the NO<sub>2</sub><sup>-</sup> oxidation to the produced <sup>30</sup>N<sub>2</sub> ratio. A ratio  
158 near the 3:1 stoichiometry of dismutation (3 NO<sub>3</sub><sup>-</sup>: 1 N<sub>2</sub>, Eq. (R4)) would indicate that  
159 dismutation could explain the NO<sub>2</sub><sup>-</sup> oxidation measured in the ODZ core.



164 A final area of OMZ biogeochemistry that we investigate is the relative balance between  
165 anammox and denitrification and these pathways' relationships to the rapid NO<sub>2</sub><sup>-</sup> oxidation /

166  $\text{NO}_3^-$  reduction loop. After the discovery of anammox, many OMZ studies (Kalvelage et al.,  
167 2013; Kuypers et al., 2005; Hamersley et al., 2007; Jensen et al., 2011; Thamdrup et al., 2006;  
168 Lam et al., 2009), but not all (Ward et al., 2009; Bulow et al., 2010; Dalsgaard et al., 2012) have  
169 reported that anammox is the dominant N loss flux in OMZs, a surprising difference from the  
170 stoichiometric based prediction that OMZ N loss should be at most 29% anammox (Dalsgaard et  
171 al., 2003). While the first wave of these studies did not realize that vial septa were introducing  
172  $\text{O}_2$  into the incubations, many studies after this discovery observed the same result (Kalvelage et  
173 al., 2013; Jensen et al., 2011; Babbin et al., 2020). Theis prediction of a 29% anammox partition  
174 assumes that all  $\text{NH}_4^+$  for anammox was derived from remineralization of OM with a mean  
175 marine C:N ratio through complete denitrification of  $\text{NO}_3^-$  to  $\text{N}_2$  (Dalsgaard et al., 2003, 2012).  
176 Anammox rates exceeding 29% of total N loss would therefore require an additional source of  
177  $\text{NH}_4^+$  beyond current observations of denitrification and the resulting  $\text{NH}_4^+$  remineralization.

178 The best supported explanations for elevated anammox are that (1) denitrification is the  
179  $\text{NH}_4^+$  source, but that complete denitrification peaks episodically in response to OM quality  
180 while anammox occurs at a slow, consistent, low rate (Ward et al., 2008; Thamdrup et al., 2006;  
181 Babbin et al., 2014; Dalsgaard et al., 2012). The snapshots afforded by isotopic incubations on  
182 cruises could therefore easily miss episodes of high complete denitrification. (2) Denitrifiers  
183 have a strong preference for particles (Ganesh et al., 2013, 2015; Fuchsman et al., 2017) and  
184 CTD samples do not capture marine particles very well (Suter et al., 2017). As a result,  
185 differences from the expected percent N loss partition in water column samples are due to  
186 missing denitrifiers. (32) The rapid loop between  $\text{NO}_3^-$  and  $\text{NO}_2^-$  described previously  
187 functions as an “engine” to generate  $\text{NH}_4^+$  for anammox at the expense of denitrification. The  
188 observed magnitudes of  $\text{NO}_3^-$  reduction and  $\text{NO}_2^-$  oxidation and these processes’ ability to

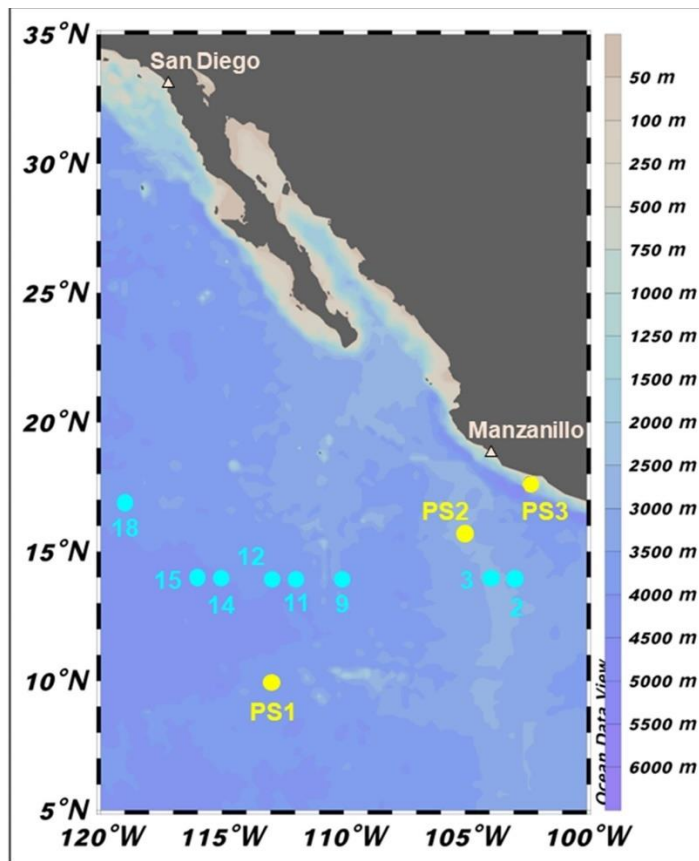


189 produce  $\text{NH}_4^+$  from the remineralization of OM with standard C:N ratios without complete  
190 denitrification make this an additional logical hypothesis.

191 The ~~third~~<sup>second</sup> hypothesis, the  $\text{NO}_2^-/\text{NO}_3^-$  loop, is supported by several pieces of  
192 evidence. ~~Firstly, such as (1) measurements that the  $\text{O}_2$  tolerance of  $\text{NO}_3^-$  reduction and~~  
193 ~~anammox is higher than that of denitrification and that therefore these processes are more adapted~~  
194 ~~to the oxycline and ODZ top (Kalvelage et al., 2011; Jensen et al., 2008; Dalsgaard et al., 2014).~~  
195 ~~Additionally, (2) 'omics studies have revealed widespread incomplete, modular denitrification in~~  
196 ~~OMZs (Sun et al. and Ward, 2021b; Ganesh et al., 2015; Fuchsman et al., 2017), and (3)~~  
197 ~~experimental~~ Furthermore, experimental studies have shown that as  $\text{NO}_3^-$  reduction increases near  
198 the coast, anammox rates also increase (Kalvelage et al., 2013). ~~According to this view, partial~~  
199 ~~denitrification of  $\text{NO}_3^-$  to  $\text{NO}_2^-$  at a much higher rate than complete denitrification would~~  
200 ~~produce  $\text{NH}_4^+$  that would then enhance anammox rates. The resulting enhanced anammox rates~~  
201 ~~occur at the expense of complete denitrification because high  $\text{NO}_3^-$  reduction rates would~~  
202 ~~consume OM before the later steps of denitrification. In addition, the resulting  $\text{NO}_2^-$  would also~~  
203 ~~be lost to later stage denitrifiers due to high  $\text{NO}_2^-$  oxidation rates that would return the  $\text{NO}_2^-$  to~~  
204  ~~$\text{NO}_3^-$ .~~ Our study's considerable number of data points, as well as our ability to compare results  
205 to rate measurements obtained from identical methods on previous cruises offers a unique chance  
206 to test both the variable denitrification and rapid loop hypotheses ~~further validate these~~  
207 ~~explanations~~ for elevated anammox rates.

208 OMZs are essential regions for the marine N cycle; however, the biogeochemistry of  
209 OMZs may currently be in flux due to anthropogenic pressures. Observational studies have  
210 reported decreases in  $\text{O}_2$  across the Pacific (Ito et al., 2017) and the expansion of denitrification  
211 and anoxia in the ETNP (Horak et al., 2016). Modelings studies and observations suggest that

212 OMZ volume will continue to grow in the near future, with uncertain impacts (Stramma et al.,  
213 2008; Keeling et al., 2010; Busecke et al., 2022). As a result, it is important to develop a  
214 thorough understanding of OMZ N cycling to be able to predict any changes in marine  
215 productivity as deoxygenated regions grow. This study contributes towards this goal through  
216 examining four open research questions in OMZ biogeochemistry:  
217 (1) Is the rapid cycle hypothesis correct, i.e., that  $\text{NO}_3^-$  reduction and  $\text{NO}_2^-$  oxidation rates are  
218 much greater than N loss rates, especially in the oxycline and ODZ top?  
219 (2) Does truly anaerobic  $\text{NO}_2^-$  oxidation occur in OMZ regions?  
220 (3) If yes, is  $\text{NO}_2^-$  dismutation the mechanism by which it occurs?  
221 (4) Is anammox the dominant N loss flux? If yes, what is the explanation?



222

223 **Figure 1:** Sampling locations during 2018 cruises to the ETNP OMZ. SR1805 stations (spring  
224 2018) are shown in yellow while FK180624 (summer 2018) stations are shown in cyan. Stations

225 PS1 and 18 are located in more oxic environments on the boundary of the OMZ region. The  
226 remaining FK180624 stations occur along a gradient towards the center of the OMZ region,  
227 represented by stations PS2 and FK180624 stations 2 and 3. These three stations are referred to  
228 as OMZ core stations. Station PS3 (referred to as coastal) represents a final biogeochemical  
229 subregion due to its proximity to the coast.

230

## 231 **2. Methods**

### 232 **2.1 NO<sub>2</sub><sup>-</sup>, NO<sub>3</sub><sup>-</sup>, and NH<sub>4</sub><sup>+</sup> concentration measurements**

233 Nutrient measurements on all cruises were conducted as follows. Ambient NO<sub>2</sub><sup>-</sup>  
234 concentrations were measured on each vessel using the sulfanilimide and NED colorimetric  
235 technique with a spectrophotometer (Strickland and Parsons, 1972). NO<sub>3</sub><sup>-</sup> profile samples were  
236 frozen onboard each ship, then thawed and measured immediately ~~NO<sub>3</sub><sup>-</sup> was measured in the~~  
237 ~~NO<sub>2</sub><sup>-</sup> oxidation experiments~~ using the chemiluminescence method upon return to the Ward  
238 laboratory (Braman and Hendrix, 1989). Ambient NH<sub>4</sub><sup>+</sup> concentrations were measured on each  
239 ship using the OPA method (Holmes et al., 1999; Taylor et al., 2007; ASTM International,  
240 2006). In some cases, NO<sub>2</sub><sup>-</sup> and NH<sub>4</sub><sup>+</sup> were measured on different casts than those of the rate  
241 measurements. In these cases, figures and calculations use interpolated nutrient values based on  
242 the potential density of nutrient sampling and rate measurement depths. Interpolations were  
243 performed with the Matlab pchip function.

### 244 **2.2 NH<sub>4</sub><sup>+</sup> oxidation and NO<sub>3</sub><sup>-</sup> reduction rates**

245 Incubation experiments were performed on board the R/V *Sally Ride* in March and April  
246 2018 (SR1805). NH<sub>4</sub><sup>+</sup> oxidation and NO<sub>3</sub><sup>-</sup> reduction rates were measured at three stations: PS1  
247 (open ocean OMZ boundary), PS2 (open ocean, OMZ), and PS3 (coastal OMZ) (Fig. 1). Rates  
248 were measured throughout the water column at ten depths per station (see supplemental Table S1  
249 for depths). Water was directly sampled from the CTD into 60\_-mL serum vials. After  
250 overflowing three times, bottles were sealed with a rubber stopper and crimped with an

251 aluminum seal. After this, a 3 mL headspace of He was introduced and samples from below the  
252 oxygenated surface depths were purged for 15 min with He at a flow rate of 0.4 L min<sup>-1</sup>. This  
253 flow rate exchanged the volume of each bottle one hundred times. ~~;~~ Immediately after this, and  
254 ~~then~~ 0.1 mL of tracer solution was added to all bottles. <sup>15</sup>NH<sub>4</sub><sup>+</sup> and <sup>15</sup>NO<sub>3</sub><sup>-</sup> tracers were added to  
255 reach final concentrations of 0.5 μM and 3 μM, respectively. Five bottles were incubated per  
256 time course and incubations were ended at 0 (one bottle), 12, and 24 hours (two bottles each) via  
257 addition of 0.2 mL of saturated ZnCl<sub>2</sub>. Samples were analyzed at the University of Basel using a  
258 custom-built gas bench connected by a Conflow IV interface to a Delta V plus IRMS (Thermo  
259 Fisher Scientific). Five mL of the sample were used to convert NO<sub>2</sub><sup>-</sup> to N<sub>2</sub>O using the azide  
260 method (McIlvin and Altabet, 2005). A linear increase of <sup>15</sup>N-NO<sub>2</sub><sup>-</sup> over time, along with a  
261 standard curve to convert from peak area units to nmol N was used to calculate the NO<sub>2</sub><sup>-</sup>  
262 production rates according to Eq. (5) and (6) below,

263 Ammonium oxidation rate =  $\frac{d \text{ }^{15}\text{NO}_2^-}{dt (F_{\text{NH}_4^+})}$  (5)

264 Nitrate reduction rate =  $\frac{d \text{ }^{15}\text{NO}_2^-}{dt (F_{\text{NO}_3^-})}$  (6)

265 where:

266  $\frac{d \text{ }^{15}\text{NO}_2^-}{dt}$  is the slope of <sup>15</sup>NO<sub>2</sub><sup>-</sup> produced over time and

267 F<sub>NH<sub>4</sub><sup>+</sup></sub> and F<sub>NO<sub>3</sub><sup>-</sup></sub> are the fraction of the NO<sub>3</sub><sup>-</sup> and NH<sub>4</sub><sup>+</sup> pools that are labelled with <sup>15</sup>N.

268 The significance of the rates was evaluated using a Student's t test with a significance level of  
269 0.05. The reported error bars are the standard error of the regression. The NH<sub>4</sub><sup>+</sup> oxidation rates  
270 reported here were previously published and the experimental method used is more thoroughly  
271 described in this previous publication (Frey et al., 2022).

272

### 273 **2.3 Anammox and denitrification rates depth profiles**

274 Incubation experiments were performed during SR1805 in March and April 2018 and on  
275 the R/V *Falkor* (FK180624) during June and July 2018. As above, rates were measured at PS1,  
276 PS2, and PS3 at ten depths per station (see Supplementary Table S1 for sampling depths) during  
277 SR1805. On FK180624, rates were measured at eight stations that spanned a gradient from the  
278 core of the OMZ region to its edges (see Supplementary Table S2 for sampling depths). At all  
279 stations and depths water was directly sampled from the CTD into 320 mL borosilicate ground  
280 glass stoppered bottles. After overflowing three times, bottles were stoppered with precision  
281 ground glass caps specifically produced to prevent gas flow. The bottles were transferred to a  
282 glove bag and amended with the following treatments: 3  $\mu\text{M}$  each of  $^{15}\text{NO}_2^-$  and  $^{14}\text{NH}_4^+$   
283 (denitrification and anammox) and 3  $\mu\text{M}$  each of  $^{15}\text{NH}_4^+$  and  $^{14}\text{NO}_2^-$  (anammox) on SR1805.

284 ~~Two~~  $\mu\text{M}$  amendments of  $^{15}\text{NO}_2^-$  and  $^{14}\text{NH}_4^+$  were used on FK180624. It should be noted that at  
285 many depths our tracer additions were far above in situ values. Due to this, all anammox and  
286 denitrification rates with high changes from baseline nutrient concentrations represent potential  
287 rates.— Eight mL of tracer amended seawater was aliquoted into 12 mL exetainers (Labco).  
288 Exetainers were sealed in a glove bag with butyl septa and plastic screw caps that had been  
289 stored under helium for at least one month, removed and then purged for 5 min at 3 psi with  
290 helium gas to remove any  $\text{O}_2$  that accumulated during sampling and processing. This step is  
291 another reason our ~~As a result of this step, it should be noted that all~~ anammox and  
292 denitrification rates sourced from partially or fully oxygenated waters should be regarded as  
293 ~~represent~~ potential rates.

294 Rates for each sampled depth were calculated using a five-timepoint time course with  
 295 three replicates at each point. Incubations were ended by injecting 50  $\mu\text{L}$  saturated  $\text{ZnCl}_2$  and  
 296 vials were stored upside down to prevent the headspace from leaking through the vial cap  
 297 ~~during~~ storage and transit. Six months after the cruise, samples were analyzed using a Europa  
 298 22-20 IRMS (Sercon). Raw data values were corrected for instrument drift due to run position  
 299 and total  $\text{N}_2$  mass. Drift corrected values and standard curves to convert from peak area units to  
 300  $\text{nmol N}_2$  were used to calculate rates according to the equations below (Thamdrup et al., 2006;  
 301 Thamdrup and Dalsgaard, 2000, 2002) (for more details see supplemental material),

302 Denitrification (from  $^{15}\text{NO}_2^-$ )

$$303 \text{ Denitrification Rate} = \frac{d \text{ }^{30}\text{N}_2}{dt(F_{\text{NO}_2^-})^2} \quad (7)$$

304 Anammox (from  $^{15}\text{NO}_2^-$ )

$$305 \text{ Anammox Rate} = \frac{d \text{ }^{29}\text{N}_2}{dt F_{\text{NO}_2^-}} - 2D(1 - F_{\text{NO}_2^-}) \quad (8)$$

306 Anammox (from  $^{15}\text{NH}_4^+$ )

$$307 \text{ Anammox Rate} = \frac{d \text{ }^{29}\text{N}_2}{dt F_{\text{NH}_4^+}} \quad (9)$$

308 where:

309  $\frac{d \text{ }^{30 \text{ or } 29}\text{N}_2}{dt}$  is the slope of the regression of the amount of  $^{30 \text{ or } 29}\text{N}_2$  vs. time,

310  $F_{\text{NO}_2^-}$  and  $F_{\text{NH}_4^+}$  are the fraction of the  $\text{NO}_2^-$  and  $\text{NH}_4^+$  pools labelled as  $^{15}\text{N}$ , and

311  $D$  is the denitrification rate calculated according to Eq. (7).

312 A Student's  $t$  test with a significance level of 0.05 was used to evaluate all rates. The reported

313 error bars are the standard error of the regression. Since the anammox rates measured via both

314 tracers on the SR1805 cruise were similar in magnitude (Supplementary Table S3), anammox  
315 values reported in Figs. 2, 3, 6, 7, 8, and 9 are based on a combination of these values (see  
316 supplementary material for more information). Previously published (Babbin et al., 2020)  
317 anammox and denitrification rates are sourced from four stations occupied during the R/V  
318 *Thomas G. Thompson*'s March and April 2012 cruise to the ETNP (TN278) and the RVIB  
319 *Nathaniel B. Palmer*'s June and July 2013 ETSP cruise (NBP1305) and were conducted in the  
320 same manner as the SR1805 and FK180624 incubations. Crucially, the same mass spectrometer  
321 was used to measure N loss rates across the 2012, 2013, and 2018 cruises. Station locations for  
322 the 2012 and 2013se cruises were as follows: TN278 ETNP coastal (20° 00' N, 106° 00' W),  
323 ETNP offshore (16° 31' N, 107° 06' W) and NBP1305 ETSP coastal (20° 40' S, 70° 41' W),  
324 ETSP offshore (13° 57' S, 81° 14' W).

325

#### 326 **2.4 SR1805 NO<sub>2</sub><sup>-</sup> oxidation depth profiles**

327 Nitrite oxidation depth profiles were measured in the same exetainers used to measure  
328 anammox and denitrification depth profiles (<sup>15</sup>NO<sub>2</sub><sup>-</sup> treatment only). The rate of NO<sub>2</sub><sup>-</sup> oxidation  
329 was determined by converting the NO<sub>3</sub><sup>-</sup> produced during the incubations to N<sub>2</sub>O using the  
330 denitrifier method (Weigand et al., 2016; Granger, J., & Sigman, 2009) (see supplemental  
331 material for methods details). The samples were stored at room temperature in the dark until  
332 analysis on a Delta V (Thermo Fisher Scientific) mass spectrometer that measures the isotopic  
333 content of N in N<sub>2</sub>O (Weigand et al., 2016). Samples were corrected for instrument drift due to  
334 run position and total N<sub>2</sub> mass (for more details see supplemental materials). Drift corrected  
335 δ<sup>15</sup>N values and a standard curve were then used to calculate the rate as follows,

336 
$$\frac{^{15}\text{N}}{^{14}\text{N}} = \frac{\left[ \frac{\delta^{15}\text{N}}{1000} + 1 \right] \times 0.003667}{1 - 0.003667}$$
 (10)

337 
$$\text{NO}_2^- \text{ ox. rate} = \frac{d \left[ ^{44}\text{N}_2\text{O}_{\text{area}} \times \frac{^{15}\text{N}}{^{14}\text{N}} \right]}{dt F_{\text{NO}_2^-}}$$
 (11)

338 where Eq. (10) is a rearrangement of the definition of  $\delta^{15}\text{N}$ :

339 
$$\delta^{15}\text{N} = \left[ \frac{\frac{^{15}\text{N}}{^{14}\text{N}}_{\text{sample}}}{\frac{^{15}\text{N}}{^{14}\text{N}}_{\text{air}}} - 1 \right] \times 1000$$
 (12)

340 and  $^{44}\text{N}_2\text{O}_{\text{area}}$  is the amount of  $^{44}\text{N}_2\text{O}$  measured as sample peak area in  $\text{V} \cdot \text{sec}$ . 0.003667 is the  
 341 natural abundance of  $^{15}\text{N}$  in air. A Student's t test with a significance level of 0.05 was used to  
 342 evaluate all rates. Reported error bars are the standard error of the regression. Previously  
 343 published (Babbin et al., 2020)  $\text{NO}_2^-$  oxidation rates are from the previously mentioned TN278  
 344 and NBP1305 cruises and were conducted at the same four stations where N loss rates were  
 345 measured. These  $\text{NO}_2^-$  oxidation rate measurements were conducted according to the same  
 346 procedures used for the SR1805 depth profiles.

347

## 348 **2.5 $\text{NO}_2^-$ oxidation and $\text{O}_2$ manipulation experiments**

349 Experiments were conducted during cruises SR1805 and FK180624 in spring and  
 350 summer 2018. Wide-mouthed Pyrex round media bottles (800 mL total volume, 500 mL  
 351 working volume; Corning, USA; product code 1397-500) were used for all incubations. These  
 352 bottles were modified to include three stainless steel bulkhead fittings (Swagelok, USA) secured  
 353 to the interior of the lid with a Viton rubber gasket and stainless-steel washer between the lid and  
 354 the sealing nut. The three ports consisted of two one-eighth inch fluidic ports (inflow and



355 outflow) and one one-quarter inch sampling port. The fluidic ports were fitted with one-eighth  
356 inch nylon tubing, with the inflow line penetrating to the base of the bottle. The one-quarter inch  
357 sampling port had a butyl rubber septum between the Swagelok stem and nut. This setup  
358 permitted *continuous* gas purging of the bottles while maintaining an otherwise closed system.

359 For each depth and O<sub>2</sub> treatment, three bottles were filled to 500 mL with sample water  
360 from a Niskin bottle and closed. Sample water for all experiments except station 18 on the  
361 FK180624 cruise was drawn from water below 2.2 μM O<sub>2</sub> (See Table S4 for all ambient O<sub>2</sub>  
362 values). Highly precise digital mass flow controllers (Alicat) were then used to establish the  
363 desired O<sub>2</sub> concentrations in each bottle. Mixing ratios were calculated to create a range of O<sub>2</sub>  
364 concentrations spanning 1 nM, 10 nM, 100 nM, 1 μM, and 10 μM. The gas mixture modified by  
365 the mass flow controllers was a zero-air gas mixture (Airgas) consisting of 21% O<sub>2</sub> and 79% N<sub>2</sub>  
366 and 1000 ppm pCO<sub>2</sub> (the approximate in situ value). Initial gas flow was 1 L min<sup>-1</sup> for 1 hour to  
367 equilibrate the seawater followed by 100 mL min<sup>-1</sup> for the remainder of the experiment. Bottles  
368 were daisy-chained together to maintain the same flow rate among them (two bottles on SR1805,  
369 six on FK180624). As in the depth profile experiments, 3 μM <sup>15</sup>NO<sub>2</sub><sup>-</sup> amendments were added  
370 prior to purging. Incubations were conducted in the dark at 12°C in a cold room (SR1805) or  
371 beverage cooler (FK180624). At the beginning of the experiments, after purging for one hour,  
372 O<sub>2</sub> was checked with a LUMOS optode with a detection limit of 0.5 nM (Lehner et al., 2015) and  
373 CO<sub>2</sub> was checked by measuring pH using the colorimetric meta-cresol purple method. The  
374 LUMOS optode confirmed that O<sub>2</sub> concentrations were within a few nM of the calculated values.  
375 While our use of high precision digital mass flow controllers and this qualitative O<sub>2</sub> check  
376 provide confidence that our O<sub>2</sub> concentrations are accurate, due to the fact that O<sub>2</sub> was not  
377 continuously monitored through the time course, we refer to each O<sub>2</sub> concentration as a

378 “putative” concentration for the remainder of this manuscript. Samples (50 mL) were withdrawn  
379 every 12 hours for two days with a four inch hypodermic needle attached to a 60 mL disposable  
380 plastic syringe. Samples were ejected into acid-cleaned HDPE bottles pre-amended with 200  $\mu$ L  
381 of saturated  $\text{ZnCl}_2$  solution. Bottles were screwed closed and wrapped with parafilm. Samples  
382 from each of the three initially collected bottles were collected to create triplicates at each time  
383 point.

384

## 385 **2.6 $\text{NO}_2^-$ dismutation experiments**

386 Nitrite dismutation experiments were performed during SR1805 at Station PS3 (coastal  
387 waters) at two deoxygenated depths: 60 m and 160 m. Incubations were performed in the same  
388 manner as the above anammox, denitrification, and  $\text{NO}_2^-$  oxidation experiments where all three  
389 rates were measured in the same exetainers. Experiments consisted of eight total treatments:  
390 four varying  $^{15}\text{NO}_2^-$  tracer concentrations (1.125, 5.25, 10.5, and 20.25  $\mu\text{M}$  for 160 m and 0.75,  
391 1.5, 3.75, and 7.5  $\mu\text{M}$  for 60 m) and two  $^{14}\text{NO}_3^-$  treatments (0 or 20  $\mu\text{M}$ ). As above, both  $^{30}\text{N}_2$   
392 and  $\text{NO}_3^-$  production via the denitrifier method (Weigand et al., 2016) were measured. In order  
393 to test our hypothesis that, if dismutation is occurring, the unexplained  $\text{NO}_2^-$  oxidation rate (the  
394 difference between the measured  $\text{NO}_2^-$  oxidation and the  $\text{NO}_2^-$  oxidation due to anammox) and  
395 the denitrification rate (i.e. the  $^{30}\text{N}_2$  production rate) should have a 3:1 ratio, a previously  
396 published anammox stoichiometry (Eq. (4) (Kuenen, 2008)) was used to calculate the  $\text{NO}_2^-$   
397 oxidation due to anammox. The anammox rates used for this calculation are included in the  
398 supplementary material (Fig. S4).

399

## 400 **2.7 Calculation of N loss from $\text{NH}_4^+$ oxidation**

401 The calculation of the maximum possible N loss from  $\text{NH}_4^+$  oxidation via NO  
402 disproportionation by ammonium oxidizing archaea (AOA) in Supplementary Table S55 was  
403 carried out by dividing the measured  $\text{NH}_4^+$  oxidation rate by two in accordance with the  
404 stoichiometry of  $\text{NH}_4^+$  oxidation and NO disproportionation proposed in a previous study (Kraft  
405 et al., 2022). It should be noted that this operation represents the extreme case where all  $^{15}\text{NO}_2^-$   
406 produced in  $\text{NH}_4^+$  oxidation is converted to  $\text{N}_2$ . We acknowledge this as an unrealistic  
407 assumption used to evaluate the extreme limits of the amount of total N loss attributable to  $\text{NH}_4^+$   
408 oxidation. This operation was carried out for all depths where  $\text{NH}_4^+$  oxidation, anammox, and  
409 denitrification rates were measured, irrespective of  $\text{O}_2$  concentration.

410

## 411 **2.8 Redundancy analysis (RDA), Principle component analysis (PCA), and statistics**

412 All RDA, PCA, redundancy, and correlation analyses were performed with the available  
413 packages in R (v4.2.1 “Funny-Looking Kid”) (R: A language and environment for statistical  
414 computing). All data were first normalized around zero before calculating the Pearson’s  
415 correlation coefficient. Gene abundances (*nirS* and *amoA*) [from qPCR analyses](#) used for the  
416 RDA and correlation analyses were measured as previously described (Peng et al., 2015;  
417 Jayakumar et al., 2009; Tang et al., 2022).

418

## 419 **2.9 Definition of shallow boundary and ODZ core nomenclature**

420 In the results and discussion sections, results are classified as shallow boundary or ODZ  
421 core waters according to a previously published threshold (Babbin et al., 2020) where shallow  
422 boundary samples have an in situ potential density  $< 26.4$ . This method is based on a global  
423 profile of OMZ waters meant to delineate shallow boundary samples as waters that are oxic or

424 may be influenced by O<sub>2</sub> intrusions (the surface, the oxycline, and the ODZ top) from those that  
 425 are not normally influenced by O<sub>2</sub> intrusions (ODZ core). Due to the fact that the potential  
 426 density threshold is based on a global average, a few depths that are clearly in the deep oxycline  
 427 based on the SR1805 O<sub>2</sub> depth profiles are classified as ODZ core ( $\sigma_\theta > 26.4$ ) by the potential  
 428 density threshold. Despite this caveat we used this naming scheme throughout the remainder of  
 429 the manuscript to enable comparisons to previous literature (Babbin et al., 2020). ~~It should be~~  
 430 ~~noted that a few samples labelled as ODZ core based on the above criteria are from the deep~~  
 431 ~~oxycline waters below the ODZ.~~

Depth	$\sigma_\theta$	OMZ features	O <sub>2</sub> intrusions?
Shallow boundary waters	< 26.4	Surface, oxycline, ODZ top	Yes
ODZ core	> 26.4	ODZ core	No

432  
 433 **Table 1:** Explanation of shallow boundary waters and ODZ core potential density based  
 434 nomenclature (Babbin et al., 2020).

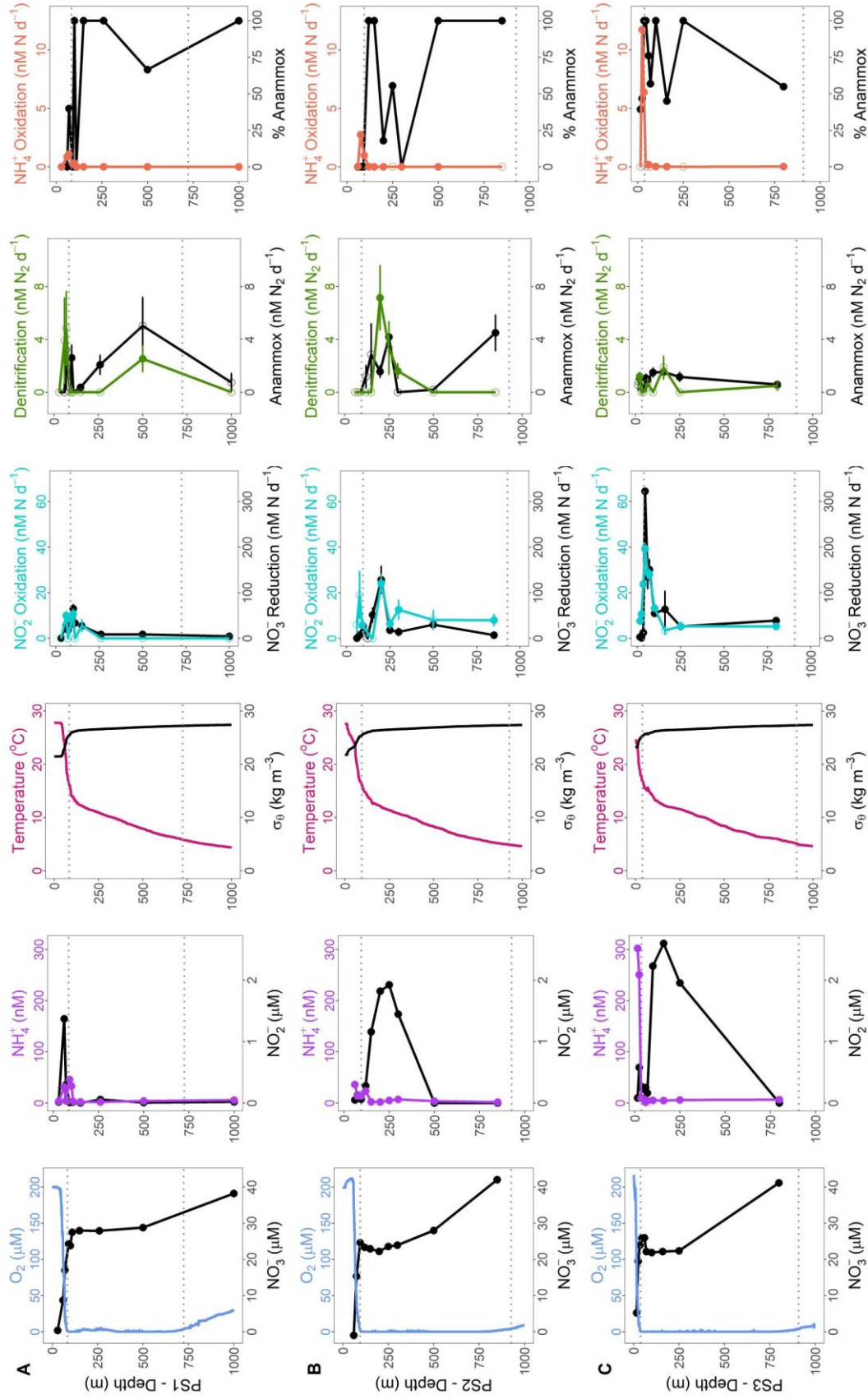
### 435 436 3. Results

#### 437 3.1 2018 depth profiles of all N cycling rates

438 N cycling depth profile experiments were conducted on two cruises (SR1805 and  
 439 FK180624) during spring and summer 2018. These two cruises sampled stations along a  
 440 gradient from the edge of the OMZ region to near the coast. Physical and chemical conditions  
 441 varied among stations PS1, PS2, and PS3 on the SR1805 cruise (spring 2018) and across all  
 442 FK180624 stations (summer 2018) (Fig. 2, Fig. S1). Broadly speaking, the vertical span of the  
 443 ODZ increased and the top of the ODZ shoaled as distance to shore decreased. Deep SNM were  
 444 observed at almost all stations with the only exceptions being the furthest offshore stations,  
 445 stations 11 and 18 from the FK180624 cruise (Fig. S1) and station PS1 from SR1805 (Fig. 2A).  
 446 Peak NO<sub>2</sub><sup>-</sup> values for all SNM were on the lower side of the range of previous ETNP  
 447 observations (Horak et al., 2016), between 1.4 – 2.6  $\mu\text{M}$ .

448           Of the five N cycling processes measured on the SR1805 cruise,  $\text{NO}_3^-$  reduction rates had  
449 the greatest magnitude at most depths. This trend was most pronounced within the upper ODZ,  
450 where  $\text{NO}_3^-$  reduction rates peaked at station PS2, and the oxycline where  $\text{NO}_3^-$  reduction rates  
451 peaked at stations PS1 and PS3 (Fig. 2). Rates of  $\text{NO}_2^-$  oxidation closely tracked  $\text{NO}_3^-$  reduction  
452 in distribution; in fact, peak  $\text{NO}_2^-$  oxidation rates co-occurred with peak  $\text{NO}_3^-$  reduction rates at  
453 all three SR1805 stations, reaching maxima of ~40 ( $\text{NO}_2^-$  oxidation) and ~300 ( $\text{NO}_3^-$  reduction)  
454 nM N d<sup>-1</sup> at PS3. However, the magnitudes of  $\text{NO}_2^-$  oxidation rates were usually lower than  
455  $\text{NO}_3^-$  reduction rates, sometimes by as much as eightfold. The third N recycling process,  $\text{NH}_4^+$   
456 oxidation, peaked at or above the oxycline, with peaks of 10 nM N d<sup>-1</sup> or less.  $\text{NH}_4^+$  oxidation  
457 was consistently measured to be zero or near-zero throughout the rest of the water column.

458



460 **Figure 2:** SR1805 depth profiles of physical parameters and N cycling rates. **(A)** From left to  
461 right,  $O_2$  ( $\mu\text{M}$ ) and  $\text{NO}_3^-$  ( $\mu\text{M}$ ) respectively in blue and black,  $\text{NH}_4^+$  (nM) and  $\text{NO}_2^-$  ( $\mu\text{M}$ )  
462 respectively in purple and black, temperature ( $^\circ\text{C}$ ) and  $\sigma_\theta$  ( $\text{kg m}^{-3}$ ) respectively in pink and black,  
463  $\text{NO}_2^-$  oxidation and  $\text{NO}_3^-$  reduction rates ( $\text{nM N d}^{-1}$ ) respectively in cyan and black, anammox  
464 and denitrification rates ( $\text{nM N}_2 \text{d}^{-1}$ ) respectively in black and green,  $\text{NH}_4^+$  oxidation rates ( $\text{nM}$   
465  $\text{N d}^{-1}$ ), and percent anammox respectively in coral and black for station PS1 (offshore). **(B)** As  
466 above but for station PS2 (OMZ). **(C)** As above but for station PS3 (coastal). Rates that are  
467 significantly different from zero are shown as filled circles, open circles signify rates not  
468 significantly different from zero. Error bars are the standard error of the regression. Grey dotted  
469 lines indicate upper and lower ODZ boundaries at the time of sampling.

470  
471 ~~all three SR1805 stations, reaching maxima of  $-40$  ( $\text{NO}_2^-$  oxidation) and  $-300$  ( $\text{NO}_3^-$  reduction)~~  
472  ~~$\text{nM N d}^{-1}$  at PS3. However, the magnitudes of  $\text{NO}_2^-$  oxidation rates were usually lower than~~  
473  ~~$\text{NO}_3^-$  reduction rates, sometimes by as much as eightfold. The third N recycling process,  $\text{NH}_4^+$~~   
474 ~~oxidation, peaked at or above the oxycline, with peaks of  $10$   $\text{nM N d}^{-1}$  or less.  $\text{NH}_4^+$  oxidation~~  
475 ~~was consistently measured to be zero or near zero throughout the rest of the water column.~~

476 Across all SR1805 and FK180624 stations, the magnitude of the N loss processes of  
477 anammox and denitrification was almost always less than  $10 \text{ nM N}_2 \text{d}^{-1}$ , a much lower magnitude  
478 than the N recycling processes of  $\text{NO}_3^-$  reduction and  $\text{NO}_2^-$  oxidation. Like  $\text{NO}_3^-$  reduction and  
479  $\text{NO}_2^-$  oxidation, the two N loss rates peaked in the upper ODZ or right at the oxycline in all three  
480 SR1805 stations, although a deep peak (850 m) in anammox was observed at station PS2 (Fig.  
481 2B). This peak occurred near the bottom of the ODZ at an  $O_2$  concentration of at station PS2  
482 (Fig. 2B).  $1.5 \mu\text{M}$ . -N loss rates also peaked near the oxycline ~~The same pattern was observed in~~  
483 ~~the three FK180624 stations with broad coverage of the ~~enough coverage of the entire~~ ODZ~~  
484 ~~water column, stations 2, 9 (6 July sampling), and 9 (9 July sampling) (Fig. S1). The relative~~  
485 ~~balance between the two N loss processes as measured by percent anammox varied widely across~~  
486 ~~the water column but largely deviated from the expected partitioning of at most 29% anammox~~  
487 ~~(Dalsgaard et al., 2003, 2012). A striking example of this is that 100% anammox values were~~

488 observed in both ODZ core and shallow boundary (see Table 1 for definitions) samples at many  
489 of the SR1805 and FK180624 stations (Fig. 2, Fig. S1).

490

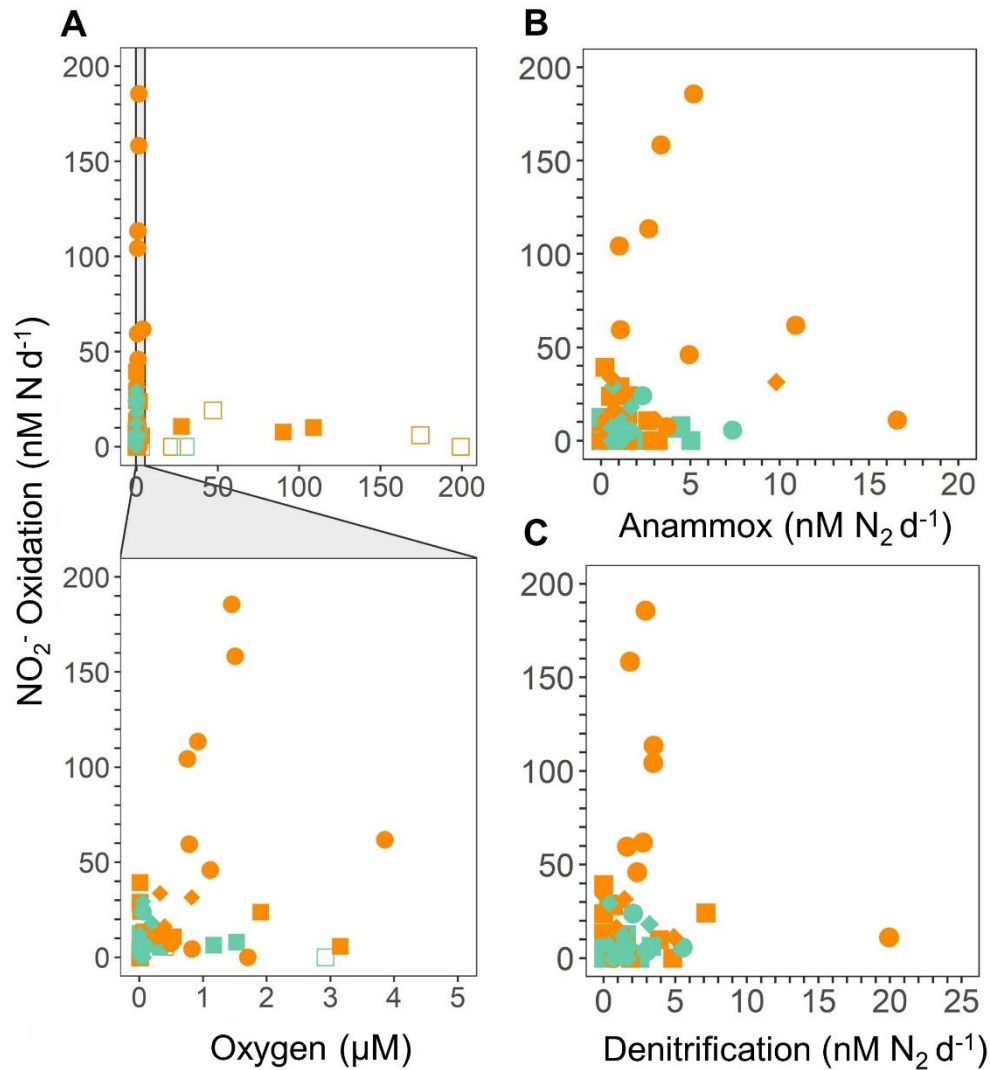
### 491 **3.2 Anaerobic NO<sub>2</sub><sup>-</sup> oxidation and O<sub>2</sub> manipulation experiments**

492 Significant NO<sub>2</sub><sup>-</sup> oxidation rates were detected in depth profiles across a range of suboxic  
493 O<sub>2</sub> concentrations (1 – 5 μM) (definition from (Berg et al., 2022)) across all SR1805 stations,  
494 often at the same depths and in the same vials where the obligately anaerobic processes of  
495 anammox and denitrification were occurring (Fig. 2, Fig. 3A-C, Fig. S2). In order to  
496 contextualize our observations, we compared our results to previously published measurements  
497 from the TN278 and NBP1305 cruises performed with identical procedures (Babbin et al., 2020).  
498 The highest rates were observed in shallow boundary waters across all three cruises (Fig. 3A-C,  
499 Fig. S2). Since low but significant levels of O<sub>2</sub> can still support aerobic NO<sub>2</sub><sup>-</sup> oxidation, a series  
500 of O<sub>2</sub> manipulation experiments was carried out on both the SR1805 (spring) and FK180624  
501 (summer) 2018 cruises (Fig. 4A-F and Fig. S3). In these experiments, ~~where the existence of~~  
502 ~~functionally~~-anoxic conditions ~~were~~ checked using a LUMOS O<sub>2</sub> optode with a detection limit  
503 of 0.5 nM (Lehner et al., 2015). ~~W~~we observed significant NO<sub>2</sub><sup>-</sup> oxidation, as well as NO<sub>3</sub><sup>-</sup>  
504 reduction at putative concentrations as low as 1 nM. Notably, compared to previous  
505 experiments, gas flushing was constant, with a refresh time of 8 min, so as to maintain O<sub>2</sub> levels  
506 within the incubation even while organisms were respiring. ~~At 1~~Below 3-nM, O<sub>2</sub> is so scarce  
507 that such waters are usually classified as functionally anoxic, ~~for example i.e. a recent review~~  
508 paper defined 3 nM as the threshold below which O<sub>2</sub> cannot play biological or biogeochemical  
509 roles (Berg et al., 2022). As a result, these experiments present convincing additional evidence



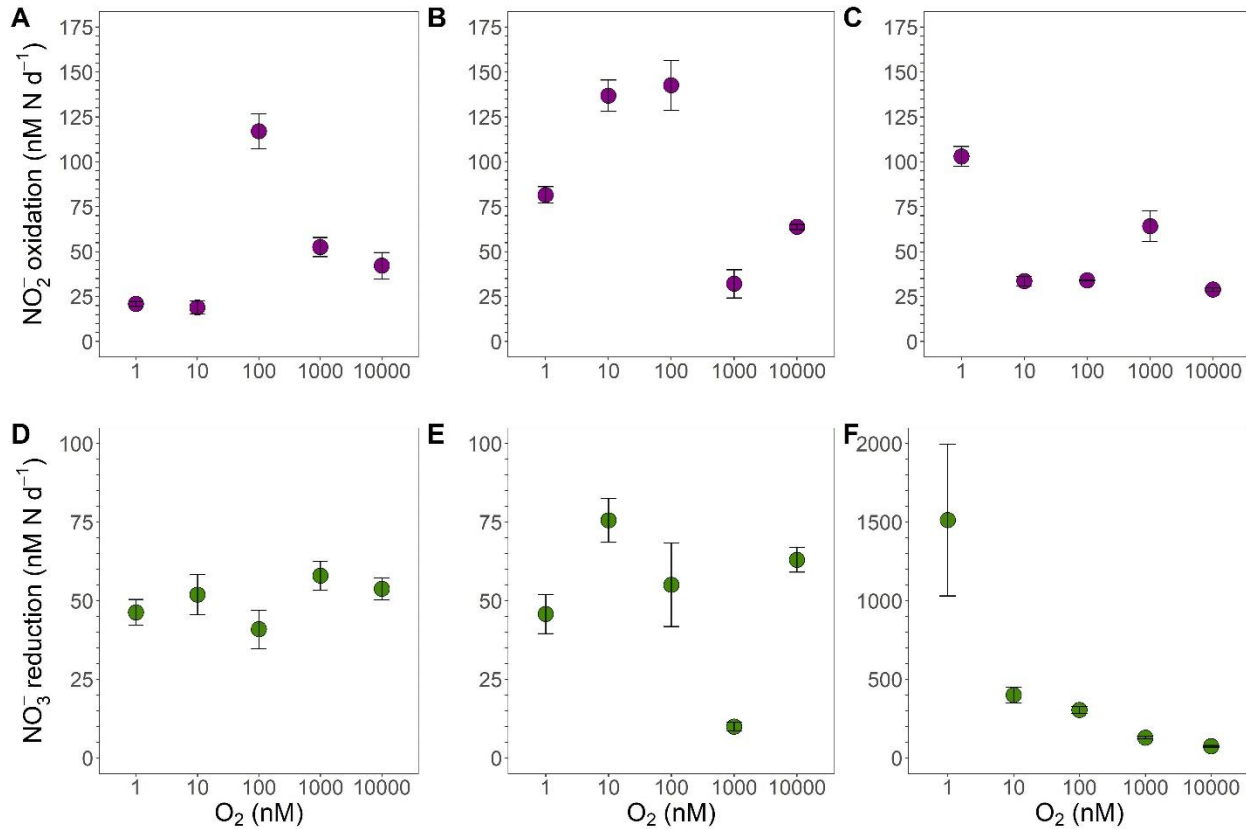
510 for the occurrence of  $\text{NO}_2^-$  oxidation up to  $\sim 100 \text{ nM N d}^{-1}$  at  $\text{O}_2$  concentrations too low to  
 511 support aerobic metabolisms.

512  
 513



514  
 515  
 516 **Figure 3:**  $\text{NO}_2^-$  oxidation rates ( $\text{nM N d}^{-1}$ ) from the 2018 SR1805 (squares), 2012 ETNP -TN278  
 517 (circles), (ETNP-2012), and 2013 ETSP NBP1305 (diamonds) ETSP-2013) cruises vs. (A)  $\text{O}_2$   
 518 concentration ( $\mu\text{M}$ ) from shipboard CTD sensors, (B) anammox rates ( $\text{nM N}_2 \text{d}^{-1}$ ), and (C)  
 519 denitrification rates ( $\text{nM N}_2 \text{d}^{-1}$ ). In A,  $\text{O}_2$  concentrations were normalized across cruises. In A,  
 520 Rates that are significantly different from zero as assessed via a Student T-test ( $p$  value  $< 0.05$ )  
 521 are displayed as filled symbols, while insignificant  $\text{NO}_2^-$  oxidation, anammox, and  
 522 denitrification rates are shown as open symbols. Rates measured in shallow boundary

523 waters are colored orange while rates from the ODZ core and below are colored teal. 2012 and  
 524 2013 data are republished (Babbin et al., 2020).  
 525



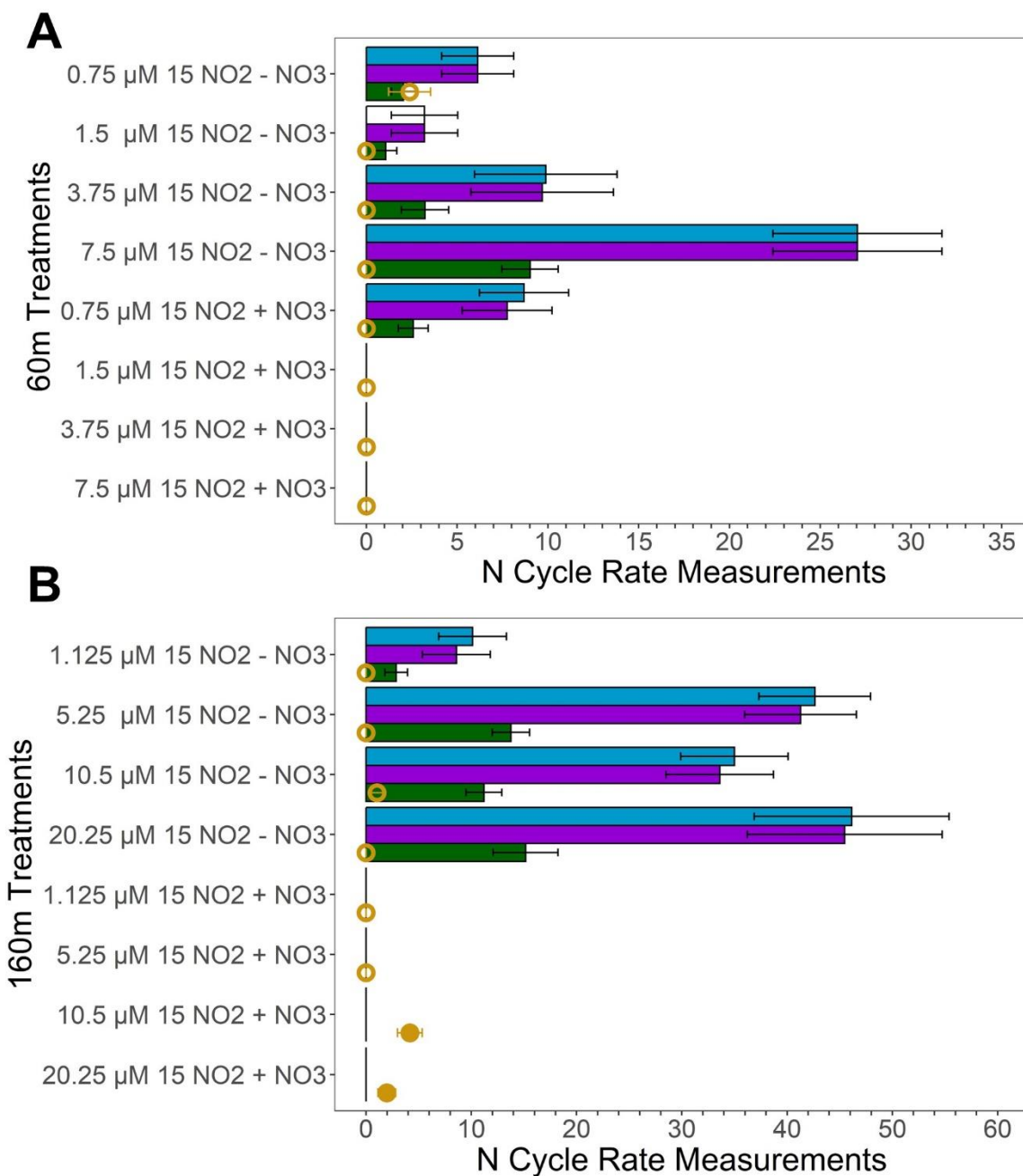
526  
 527  
 528 **Figure 4:** Oxygen manipulation experiments that show  $\text{NO}_2^-$  oxidation (purple) (A-C) and  $\text{NO}_3^-$   
 529 reduction (green) (D-F) rates ( $\text{nM N d}^{-1}$ ) measured across putative  $\text{O}_2$  concentrations from 1 to  
 530 10,000 nM during the SR1805 cruise. Experiments were conducted with waters from the ODZ  
 531 top: 93 – 110m (PS1) (A, D), 113 – 130m (PS2) (B, E), and 45 – 60m (PS3) (C, F). Error bars  
 532 are the standard error of the regression. All rates were significantly different from zero.  
 533

534  
 535 **3.3  $\text{NO}_2^-$  dismutation**

536 In order to investigate the mechanism for the observed anaerobic  $\text{NO}_2^-$  oxidation,  
 537 experiments were conducted to search for evidence of  $\text{NO}_2^-$  dismutation. If  $\text{NO}_2^-$  dismutation is  
 538 the dominant explanation for the observed anaerobic  $\text{NO}_2^-$  oxidation, we hypothesized that (1)  
 539 adding  $\text{NO}_3^-$  should suppress both  $^{30}\text{N}_2$  and  $\text{NO}_3^-$  production by LeChatelier's principle, (2)  
 540 increasing  $^{15}\text{NO}_2^-$  concentration should increase both denitrification (the  $^{30}\text{N}_2$  production rate)  
 541 and  $\text{NO}_2^-$  oxidation especially when no additional  $\text{NO}_3^-$  was added, and (3) that the ratio

542 between the “unexplained  $\text{NO}_2^-$  oxidation,” i.e., the difference between the observed  $\text{NO}_2^-$   
543 oxidation and the  $\text{NO}_2^-$  oxidation due to anammox, and the observed denitrification ( $^{30}\text{N}_2$   
544 production) rate should be close to 3:1. In experiments with He-purged water from two  
545 deoxygenated depths (60 and 160 m at station PS3, [see table S5 for  \$\text{O}\_2\$  values](#)) during the  
546 SR1805 cruise we observed that adding 20  $\mu\text{M}$   $\text{NO}_3^-$  suppressed  $\text{NO}_2^-$  oxidation across nearly all  
547 pairs [of 0 and 20  \$\mu\text{M}\$   \$\text{NO}\_3^-\$  experiments](#) -where [the  \$\text{NO}\_2^-\$  concentration](#) was identical ~~and  $\text{NO}_3^-$~~   
548 ~~varied between 0 or 20  $\mu\text{M}$   $\text{NO}_3^-$~~ -(Fig. 5). However, we did not observe a simultaneous  
549 suppression of  $\text{N}_2$  production due to the fact that the measured denitrification rate was low and  
550 insignificantly different from zero in most of our 16 treatments (Fig. 5). [The lack of an observed](#)  
551 [response in  \$\text{N}\_2\$  production could be due to already elevated ambient  \$\text{NO}\_3^-\$  concentrations, 26  \$\mu\text{M}\$](#)   
552 [and 22.2  \$\mu\text{M}\$  at 60 m and 160 m respectively. Roughly doubling the amount of  \$\text{NO}\_3^-\$  would](#)  
553 [have little effect on the denitrification rate if the relevant enzymes were already saturated, as is](#)  
554 [plausible at those concentrations.](#) As a result [of our inability to observe denitrification](#), our first  
555 hypothesis yielded little evidence of dismutation.

556 Across all four 60 m 0  $\mu\text{M}$  added  $\text{NO}_3^-$  treatments (Fig. 5A), adding  $\text{NO}_2^-$  did increase  
557  $\text{NO}_2^-$  oxidation; however, we did not observe an increase in denitrification. Surprisingly, across  
558 the four 60 m 20  $\mu\text{M}$  added  $\text{NO}_3^-$  treatments, adding  $\text{NO}_2^-$  decreased  $\text{NO}_2^-$  oxidation, the reverse  
559 of our hypothesis (Fig. 5). Across all four 160 m 0  $\mu\text{M}$  added  $\text{NO}_3^-$  treatments, we also observed  
560 an increase in  $\text{NO}_2^-$  oxidation at higher  $\text{NO}_2^-$  concentrations but did not observe an increase in  
561 the measured denitrification rate (Fig. 5B). In the four 160 m 20  $\mu\text{M}$  added  $\text{NO}_3^-$  treatments,  
562  $\text{NO}_2^-$  oxidation and denitrification did not increase with  $\text{NO}_2^-$  concentration (Fig. 5B). Due to  
563 the consistently low and insignificant denitrification rates our test of the  $\text{NO}_2^-$  addition  
564 hypothesis also yielded little evidence for dismutation.



565

566 **Figure 5:**  $\text{NO}_2^-$  dismutation tests conducted in deoxygenated waters from 60m (A) and 160m (B)  
 567 at station PS3 during the SR1805 cruise. Measured  $\text{NO}_2^-$  oxidation rates ( $\text{nM N d}^{-1}$ ) are  
 568 displayed in blue, unexplained  $\text{NO}_2^-$  oxidation rates, the difference between the measured  $\text{NO}_2^-$   
 569 oxidation and the  $\text{NO}_2^-$  oxidation due to anammox ( $\text{nM N d}^{-1}$ ), are shown in purple. The  
 570 predicted denitrification ( $\text{nM } ^{30}\text{N}_2 \text{ d}^{-1}$ ) if all the unexplained  $\text{NO}_2^-$  oxidation was due to  $\text{NO}_2^-$   
 571 dismutation is shown in green. The measured denitrification rate ( $\text{nM } ^{30}\text{N}_2 \text{ d}^{-1}$ ) is shown in  
 572 yellow where filled circles indicate significant rates and open circles indicate rates that are not  
 573 significantly different from zero. All bars filled with colors indicate significant rates (i.e. the  
 574 white bar for the 60 m 1.5  $\mu\text{M}$   $^{15}\text{NO}_2^-$ , 0  $\mu\text{M}$   $\text{NO}_3^-$  treatment  $\text{NO}_2^-$  oxidation rate denotes an

575 insignificant rate). Error bars are the standard error of the regression for  $\text{NO}_2^-$  oxidation, or are  
576 calculated based on the rules of error propagation from the standard error of the regressions for  
577 the  $\text{NO}_2^-$  oxidation and anammox rates. (+)  $\text{NO}_3^-$  treatments received  $20 \mu\text{M } ^{14}\text{NO}_3^-$  additions  
578 while the (-)  $\text{NO}_3^-$  treatments received no addition. Anammox rates used to calculate the  
579 unexplained  $\text{NO}_2^-$  oxidation rate are shown in the supplementary material.

580  
581 We were also unable to observe evidence for the ratio hypothesis due to the paucity of  
582 significant denitrification ( $^{30}\text{N}_2$  production) rates (Fig. 5). Since denitrification rates were  
583 consistently low or insignificantly different from zero, the ratio of  $\text{NO}_2^-$  oxidation to  
584 denitrification deviated from the 3:1 ratio expected if  $\text{NO}_2^-$  dismutation accounts for most of the  
585 observed  $\text{NO}_2^-$  oxidation. The only slight exception to this is the 60 m treatment with  $0.75 \mu\text{M}$   
586  $^{15}\text{NO}_2^-$  and  $0 \mu\text{M}$  added  $\text{NO}_3^-$ , the treatment closest to in situ conditions. In this treatment, the  
587 measured denitrification rate, while insignificantly different from zero on the basis of the p value  
588 of the regression, agrees with the predicted denitrification rate based on the 3:1 stoichiometry of  
589 dismutation. While our dismutation experiments as a whole suggest that  $\text{NO}_2^-$  dismutation is not  
590 a likely explanation for observed anaerobic  $\text{NO}_2^-$  oxidation, results from the 60 m  $0.75 \mu\text{M}$   
591  $^{15}\text{NO}_2^-$ ,  $0 \mu\text{M}$   $\text{NO}_3^-$  treatment provide slight justification to continue tests of this hypothesis.

592

## 593 **4. Discussion**

### 594 **4.1 Rapid $\text{NO}_2^- / \text{NO}_3^-$ cycle**

595 Depth profiles of N transformation rates obtained on the SR1805 cruise show that the  
596 rates of  $\text{NO}_2^-$  oxidation and  $\text{NO}_3^-$  reduction are far greater than rates of the N loss processes of  
597 anammox and denitrification, especially in shallow boundary (see Table 1 for definition) waters  
598 (Fig. 2, Fig. 6A – B). In fact, when the combined N recycling pathways of  $\text{NO}_2^-$  oxidation and  
599  $\text{NO}_3^-$  reduction are compared to the total N loss, the N recycling pathways are 3.2 – 192.8 times  
600 larger than the total N loss. That the minimum ratio is  $\sim 3$  strongly emphasizes the

601 preponderance of  $\text{NO}_2^-$  oxidation and  $\text{NO}_3^-$  reduction above N loss processes. As expected due  
602 to the oligotrophic nature of the offshore ETNP (Fuchsman et al., 2019) ~~lower OM~~  
603 ~~concentrations offshore~~ and as previously found in an ETSP N cycling study (Kalvelage et al.,  
604 2013),  $\text{NO}_2^-$  oxidation and  $\text{NO}_3^-$  reduction generally increased from the offshore station (PS1)  
605 towards the coast. We observed  $\text{NO}_3^-$  reduction rates of a similar magnitude to previously  
606 reported ETSP studies (Kalvelage et al., 2013; Babbin et al., 2017), a finding that generalizes the  
607 predominance of  $\text{NO}_3^-$  reduction to  $\text{NO}_2^-$  to the ETNP. Thus, our work supports several recent  
608 studies (Babbin et al., 2020, 2017; Peters et al., 2016) suggesting that most nitrogen within OMZ  
609 regions is continuously recycled between  $\text{NO}_2^-$  and  $\text{NO}_3^-$  by rapid  $\text{NO}_2^-$  oxidation and  $\text{NO}_3^-$   
610 reduction, especially in shallow boundary waters.

611 A previous work (Babbin et al., 2017) predicted that  $\text{NO}_3^-$  reduction should follow a  
612 Martin curve (Martin et al., 1987) power law distribution across the water column due to its  
613 dependence on the OM flux from shallower waters. Such a distribution was observed at stations  
614 PS1 and PS3; however,  $\text{NO}_3^-$  reduction at station PS2 did not follow a classical Martin curve  
615 profile since the  $\text{NO}_3^-$  production peak is well below the oxycline. This exception could be due  
616 to zooplankton which have been observed to migrate into the ODZ on a daily basis (Bianchi et  
617 al., 2014). Due to the fact that migrating zooplankton funnel surface OM to the mesopelagic  
618 (Cram et al., 2022), such a transfer would move OM in a pattern not consistent with the Martin  
619 curve. The transferred OM could then support the observed peak in  $\text{NO}_3^-$  reduction (Fig. 2).  
620 ~~An additional interesting trend specific to station PS2 is that the deeper peak of  $\text{NO}_3^-$  reduction~~  
621 ~~coincides with a peak in complete denitrification to  $\text{N}_2$  and a steep drop in the percent of N loss~~  
622 ~~due to anammox (Fig. 2). This connection is also visible in Fig. 6B which shows that  $\text{NO}_3^-$~~   
623 ~~reduction increases with total N loss at station PS2.~~

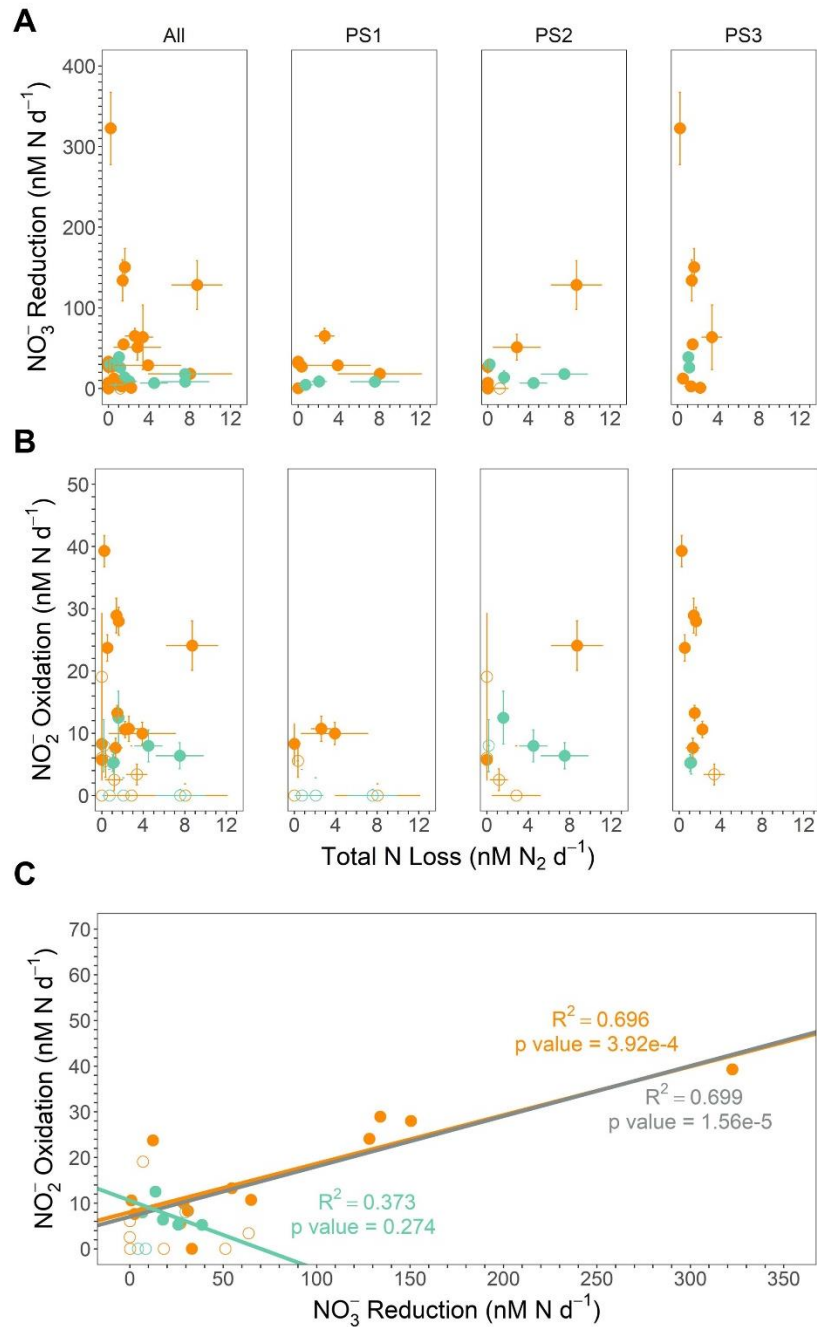
624 These results are consistent with the idea, also supported by many recent studies  
625 (Kalvelage et al., 2013; Lam and Kuypers, 2011; Lam et al., 2009; Babbin et al., 2020, 2017;  
626 Füssel et al., 2011; Lam et al., 2011), that the accumulated  $\text{NO}_2^-$  in the SNM usually results from  
627 an imbalance between  $\text{NO}_3^-$  reduction and other N cycling pathways. We further investigated  
628 this hypothesis by constructing a net  $\text{NO}_2^-$  budget derived from the five microbial N cycling  
629 metabolisms measured on the SR1805 cruise (Fig. 7). Summing the depth profiles of  $\text{NO}_2^-$   
630 consumption (anammox, denitrification, and  $\text{NO}_2^-$  oxidation) and production ( $\text{NH}_4^+$  oxidation  
631 and  $\text{NO}_3^-$  reduction) pathways revealed that net depth integrated  $\text{NO}_2^-$  production across the  
632 sampled OMZ water column depths is on the order of tens of millimoles of  $\text{NO}_2^-$  per square  
633 meter per day at all three stations (8.19 at PS1, 14.49 at PS2, and 28.97  $\text{mmol NO}_2^- \text{ m}^{-2} \text{ d}^{-1}$  at  
634 PS3). This excess  $\text{NO}_2^-$  is driven by  $\text{NO}_3^-$  reduction, which across all stations is of a much  
635 greater magnitude than all other measured N cycling processes (Fig. 2 and Fig. 7).

636 These budget calculations take the reported rates at face value, ignoring the likelihood  
637 that some of them are potential rates. For example, anammox might have been enhanced by the  
638 addition of 3  $\mu\text{M NH}_4^+$ . Denitrification is less likely to be stimulated by the addition of  $\text{NO}_2^-$ ,  
639 because it is generally limited by organic matter availability (Ward et al. 2008, Babbin et al  
640 2014). Thus, the relative importance of anammox and denitrification might be perturbed due to  
641 differential responses of the two rates to tracer additions. Analogously,  $\text{NO}_2^-$  oxidation was  
642 likely stimulated by addition of  $\text{NO}_2^-$  tracer (Sun et al. 2017), but  $\text{NO}_3^-$  reduction less so by  
643 addition of  $\text{NO}_3^-$  tracer because the latter is a heterotrophic process, and as a component of the  
644 complete denitrification pathway, likely limited by organic matter availability. These differential  
645 limitations by substrate probably mean that the calculated budget of Figure 7 is not completely  
646 accurate, but the relative importance of the processes is robust. If anything, the dominance of

647 anammox over denitrification is probably less than that observed, and the excess of  $\text{NO}_3^-$   
648 reduction over  $\text{NO}_2^-$  oxidation greater than observed. Overall, the dominance of the  $\text{NO}_3^- / \text{NO}_2^-$   
649 loop over the N loss pathways and the overwhelming importance of  $\text{NO}_3^-$  reduction are both  
650 supported by these considerations.

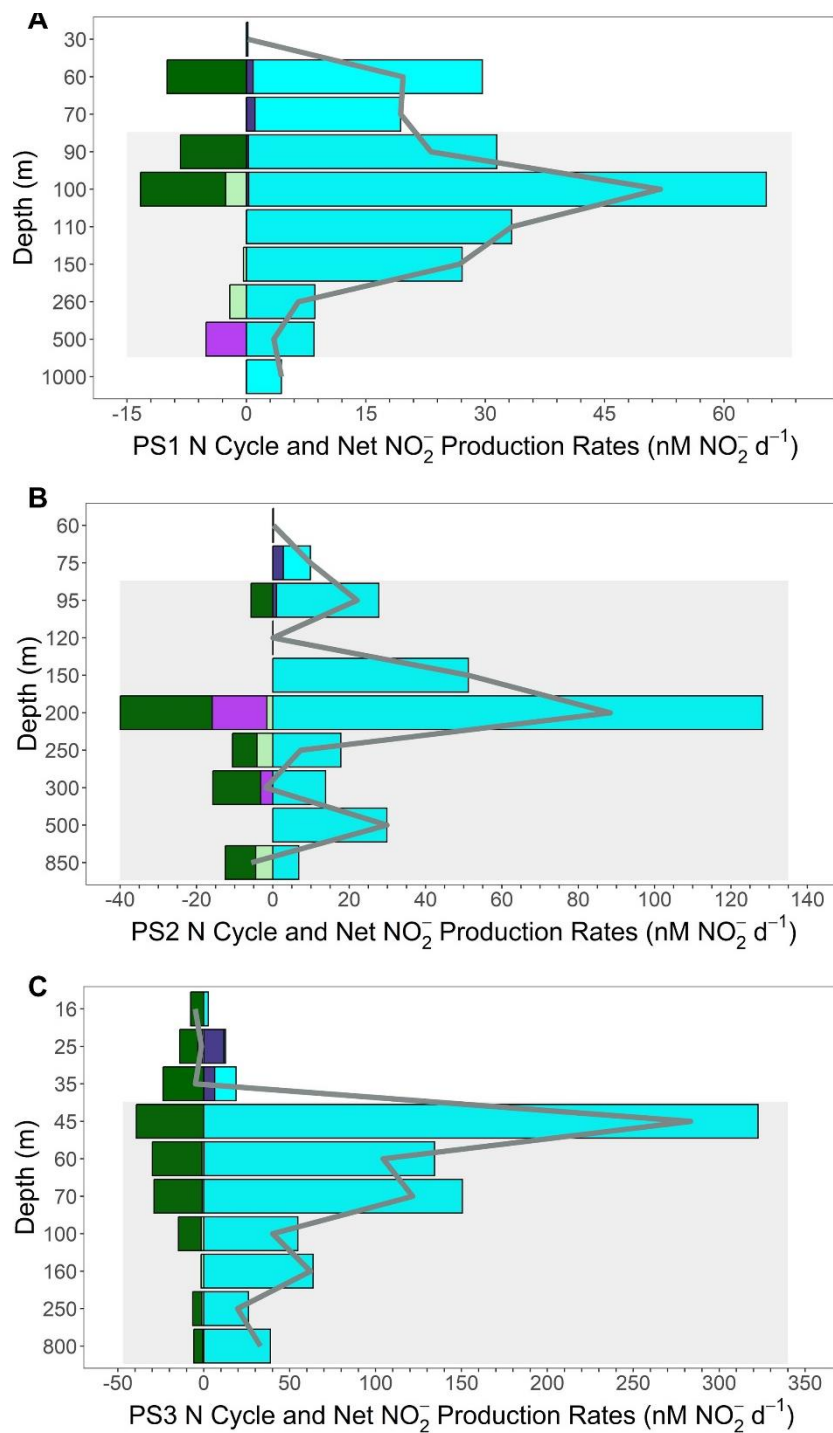
651 Additional support that  $\text{NO}_3^-$  reduction supplies the accumulated  $\text{NO}_2^-$  in the SNM can  
652 be found by comparing the net  $\text{NO}_2^-$  production rates with the measured  $\text{NO}_2^-$  concentrations  
653 along the SR1805 cruise track from offshore station PS1 to coastal station PS3. As would be  
654 expected if the SNM depended on  $\text{NO}_2^-$  derived from  $\text{NO}_3^-$  reduction, the peak net  $\text{NO}_2^-$   
655 production value across all depths at each station, the depth integrated  $\text{NO}_2^-$  production values  
656 for each station, and the magnitude of the SNM peak  $\text{NO}_2^-$  concentrations all increase together  
657 from offshore station PS1 to coastal station PS3. Importantly, we did not take into account water  
658 column mixing in both vertical and horizontal directions that would carry away produced  $\text{NO}_2^-$   
659 or  $\text{NO}_2^-$  assimilation into OM, and we recommend follow up studies that include  
660 parameterizations for these values in OMZ N Cycling modeling.





661

662 **Figure 6:** (A) NO<sub>3</sub><sup>-</sup> reduction (nM N d<sup>-1</sup>) vs. Total N loss (the sum of denitrification and  
 663 anammox in nM N<sub>2</sub> d<sup>-1</sup>) from the SR1805 cruise. (B) NO<sub>2</sub><sup>-</sup> oxidation (nM N d<sup>-1</sup>) vs. Total N loss  
 664 from the SR1805 cruise. (C) NO<sub>2</sub><sup>-</sup> oxidation vs. NO<sub>3</sub><sup>-</sup> reduction. Regression lines and statistics  
 665 are shown for the significant rates from shallow boundary waters only (orange), ODZ core  
 666 waters only (teal), and all significant data (grey). All points from shallow boundary waters are  
 667 colored orange while all points from the ODZ core or below are colored teal. Open circles  
 668 indicate points where the NO<sub>3</sub><sup>-</sup> reduction rate (A), NO<sub>2</sub><sup>-</sup> oxidation rate (B), or in (C) either NO<sub>3</sub><sup>-</sup>  
 669 reduction or NO<sub>2</sub><sup>-</sup> oxidation rate is not significantly different from zero while filled circles  
 670 indicates rates significantly different from zero.

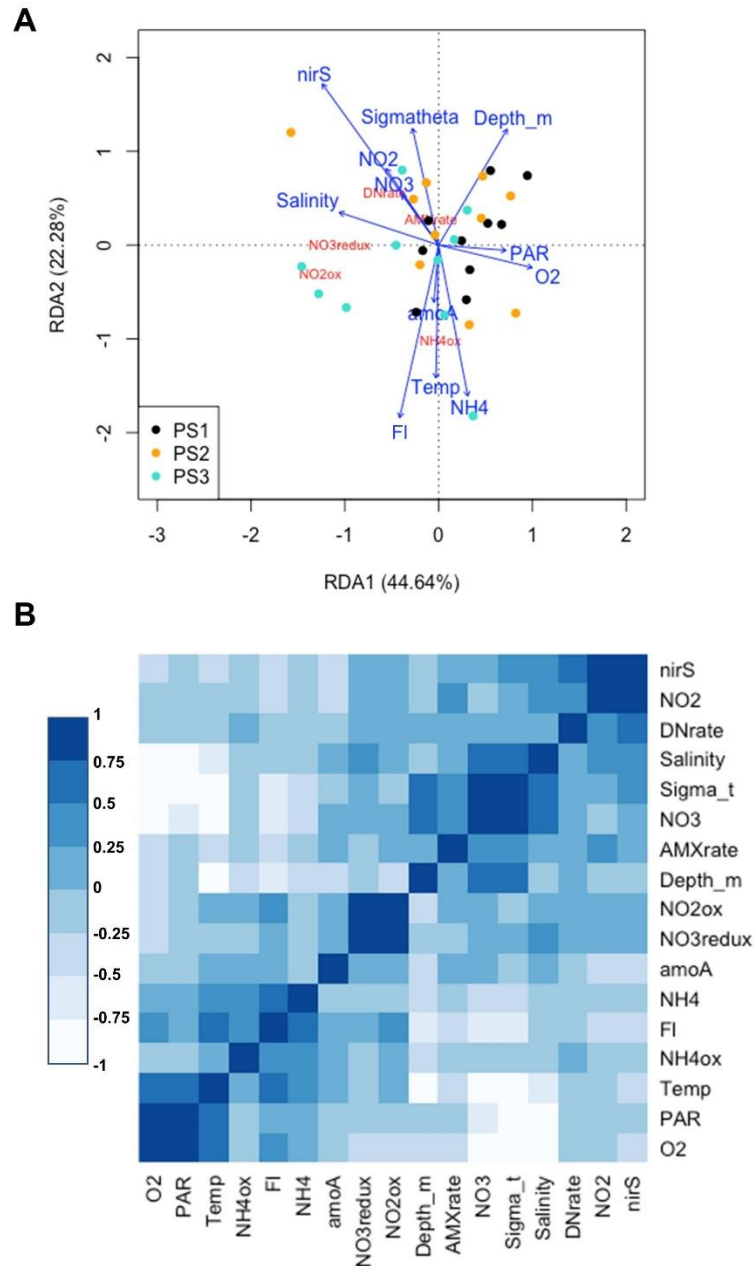


671  
672

673 **Figure 7:**  $\text{NO}_2^-$  budget profiles from the SR1805 cruise. Plots are a combination of the  $\text{NO}_2^-$   
674 production pathways of  $\text{NO}_3^-$  reduction (cyan),  $\text{NH}_4^+$  oxidation (dark purple) and the  $\text{NO}_2^-$   
675 consumption pathways of anammox (light green), denitrification (bright purple), and  $\text{NO}_2^-$   
676 oxidation (dark green). Consumption pathways are reported as negative numbers. All rates are  
677 reported in  $\text{nM NO}_2^- \text{d}^{-1}$ . The net  $\text{NO}_2^-$  production or consumption rate ( $\text{nM NO}_2^- \text{d}^{-1}$ ) is  
678 represented as a grey line for each depth. Grey boxes indicate the completely deoxygenated  
679 ODZ region at each station at the time of sampling. (A) PS1, (B) PS2, and (C) PS3.

## 680 4.2 NO<sub>2</sub><sup>-</sup> oxidation – distribution and magnitude in comparison to previous studies

681 The high rates of observed NO<sub>3</sub><sup>-</sup> reduction provide sufficient NO<sub>2</sub><sup>-</sup> to support NO<sub>2</sub><sup>-</sup>  
682 oxidation both in the oxycline and in the ODZ, as previously proposed (Anderson et al., 1982),  
683 Our observations also further confirm isotopic studies that suggested high NO<sub>2</sub><sup>-</sup> oxidation rates  
684 because rapid re-oxidation of NO<sub>2</sub><sup>-</sup> back to NO<sub>3</sub><sup>-</sup> was necessary to achieve isotopic mass balance  
685 (Buchwald et al., 2015; Casciotti et al., 2013; Granger and Wankel, 2016). Our results also align  
686 with previous experimental observations of high NO<sub>2</sub><sup>-</sup> oxidation rates (Kalvelage et al., 2013;  
687 Babbin et al., 2020; Lipschultz et al., 1990). Support for a closely connected rapid cycle  
688 between the two processes can be seen in the strong correlation between NO<sub>2</sub><sup>-</sup> oxidation and  
689 NO<sub>3</sub><sup>-</sup> reduction observed in all SR1805 cruise samples, especially those from shallow boundary  
690 waters (Fig. 6C, Fig. 8). Similarly to some previous ETSP papers (Babbin et al., 2017, 2020;  
691 Frey et al., 2020) and two ETNP studies (Peng et al., 2015; Sun et al., 2017) we observed that  
692 rates of NO<sub>2</sub><sup>-</sup> oxidation, like rates of NO<sub>3</sub><sup>-</sup> reduction, peaked in the oxycline or in the ODZ top  
693 (Fig. 2) and then declined throughout the ODZ. Unlike some stations in these studies (Babbin et  
694 al., 2020, 2017) we did not observe a second peak in NO<sub>2</sub><sup>-</sup> oxidation near the deep oxycline. In  
695 addition to observing a similar distribution, we also observed that NO<sub>2</sub><sup>-</sup> oxidation occurs at a  
696 similar magnitude to some stations in previous ETSP studies (Babbin et al., 2020, 2017; Peng et  
697 al., 2016) and ETNP (Peng et al., 2015), although our highest rates (25 – 40 nM N d<sup>-1</sup>) were  
698 much lower than the peaks measured at other stations in most of these reports (Babbin et al.,  
699 2020; Peng et al., 2015, 2016), which reached as high as ~600 nM N d<sup>-1</sup> (Peng et al., 2015;  
700 Lipschultz et al., 1990).



701

702 **Figure 8:** (A) Redundancy analysis of all environmental variables and microbial rates measured  
 703 on the SR1805 cruise. Points are color-coded by station, black (PS1), yellow (PS2), and cyan  
 704 (PS3). Variables names and arrows are color coded so that environmental variables are blue and  
 705 rate measurements are red. (B) Correlation analysis for all environmental variables and  
 706 microbial N cycle rates from the SR1805 cruise. More positive correlations are shaded to  
 707 become bluer as significance grows while negative correlations are shaded to become whiter as  
 708 significance grows. Abbreviations used are as follows: O2 (oxygen concentration normalized  
 709 across different sensors), PAR (photosynthetically active radiation normalized across sensors),  
 710 NH4ox (NH<sub>4</sub><sup>+</sup> oxidation rate), FI (chlorophyll fluorescense normalized across different sensors),  
 711 NH4 (NH<sub>4</sub><sup>+</sup> concentration), *amoA* (*amoA* abundance), NO<sub>3</sub><sup>-</sup>redux (NO<sub>3</sub><sup>-</sup> reduction rate), NO<sub>2</sub>ox

712 (NO<sub>2</sub><sup>-</sup> oxidation rate), AMXrate (anammox rate), NO<sub>3</sub><sup>-</sup> (NO<sub>3</sub><sup>-</sup> concentration), DNrate  
713 (denitrification rate), NO<sub>2</sub> (NO<sub>2</sub><sup>-</sup> concentration), and *nirS* (*nirS* abundance).

714

715

### 716 4.3 NO<sub>2</sub><sup>-</sup> oxidation – can it occur anaerobically?

717 NO<sub>2</sub><sup>-</sup> oxidation depth profiles (Figs. 2, 3) and O<sub>2</sub> manipulation experiments (Fig. 4)

718 provide further evidence that NO<sub>2</sub><sup>-</sup> oxidation can occur even when O<sub>2</sub> is as low as ~1 nM. under

719 functionally anoxic conditions. While our O<sub>2</sub> manipulation experiments provide the most

720 convincing evidence of anaerobic NO<sub>2</sub><sup>-</sup> oxidation ~~O<sub>2</sub> was not directly measured in the depth~~

721 profile experiments, several factors argue that the NO<sub>2</sub><sup>-</sup> oxidation observed in our depth

722 profile ~~these~~ incubations may be O<sub>2</sub> independent. As argued previously (Babbin et al., 2020):

723 (1) The pre-incubation He purging step in our depth profile method removes more than 99% of

724 the N<sub>2</sub> present in exetainers (Babbin et al., 2020). If it is assumed that O<sub>2</sub> is removed at identical

725 efficiency, a reasonable proposition since O<sub>2</sub> equilibrates faster than N<sub>2</sub> (Wanninkhof, 1992), the

726 introduction during sample processing of as much as 1 μM O<sub>2</sub> would result in a ~10 nM

727 contamination. As a result, if NO<sub>2</sub> oxidation is observed in samples from the deoxygenated ODZ

728 core, contamination during sampling would be kept very small by our purging step. This

729 conclusion was further validated by direct O<sub>2</sub> measurements using Lumos sensors in exetainers.

730 These tests of our purging method showed that O<sub>2</sub> was reduced to less than 10 nM in 5 minutes

731 (Sun et al. unpublished data).

732 (2) Linear timecourses across all timepoints were observed in some of our experiments,

733 including many from deoxygenated depths at station PS3 (Supplemental Figs. S7-9). If NO<sub>2</sub><sup>-</sup>

734 oxidation depended on O<sub>2</sub>, an initial acceleration (due to O<sub>2</sub> contamination that sparked NO<sub>2</sub><sup>-</sup>

735 oxidation) or later steep drop (due to the exhaustion of O<sub>2</sub> by aerobic NOB) in NO<sub>2</sub><sup>-</sup> oxidation

736 would be expected, not a consistent linear slope.

737 (3) Metagenomic evidence has revealed distinct NOB communities in oxic surface waters, the  
738 oxycline and ODZ top, and the ODZ core in OMZ regions (Sun et al., 2019). In addition we  
739 observed decreasing  $\text{NO}_2^-$  oxidation rates with increasing in situ  $\text{O}_2$  in the SR1805 incubations as  
740 well as the TN278 and NBP1305 incubations (Fig. 3A). These observations are consistent with  
741 the hypothesis that aerobic NOB from oxic depths are ill-equipped to oxidize  $\text{NO}_2^-$  in  
742 deoxygenated conditions but that the unique MAGs recently identified in draft genomes from the  
743 ODZ top and core (Sun et al., 2019), are adapted to perform anaerobic  $\text{NO}_2^-$  oxidation.

744 ~~(4) We observed  $\text{NO}_2^-$  oxidation at the same depths and often in the same incubation vessels as~~  
745 ~~the obligately anaerobic processes of anammox and denitrification (Fig. 2, Fig. 3B-C). Our~~  
746 ~~observations are consistent with several previous observations that these processes occur at the~~  
747 ~~same depths (Babbin et al., 2020; Sun et al., 2021).~~

748 (45) Through plotting  $\text{O}_2$  concentrations against the ratio between  $\text{NO}_3^-$  reduction and  $\text{NO}_2^-$   
749 oxidation at all SR1805 depths with significant, positive  $\text{NO}_2^-$  oxidation rates, we observed that  
750 the known anaerobic process of  $\text{NO}_3^-$  reduction and  $\text{NO}_2^-$  oxidation did not exhibit differential  
751 regulation by  $\text{O}_2$  as would be expected if  $\text{NO}_2^-$  oxidation was an obligately aerobic process (Fig.  
752 S5).

753 Previous studies have shown that  $\text{O}_2$  additions to purged incubations of ODZ waters can  
754 inhibit  $\text{NO}_2^-$  oxidation (Sun et al., 2017, 2021a) and that  $\text{NO}_2^-$  oxidation can occur in the absence  
755 of  $\text{O}_2$  consumption (Sun et al., 2021a). However, another kinetics study has reported  $\text{O}_2$   
756 stimulation of  $\text{NO}_2^-$  oxidation in OMZ waters (Bristow et al., 2016) and concluded that  $\text{NO}_2^-$   
757 oxidation is fundamentally an aerobic process. This apparent contradiction might be explained  
758 by several details in the experimental process of that study (Bristow et al., 2016):

759 (1) The study site is at the farthest edge of the ETSP OMZ in a location that is only anoxic in the  
760 austral summer.

761 (2) The cruise was conducted as austral summer turned to fall (March 20 – 26<sup>th</sup>), a period where  
762 O<sub>2</sub> intrusions would be more likely.

763 (3) O<sub>2</sub> data from the study's cruise (Tiano et al., 2014) show that the depths from which NO<sub>2</sub><sup>-</sup>  
764 oxidation O<sub>2</sub> kinetics samples were sourced experienced O<sub>2</sub> concentrations of 2 μM (50 m), 10  
765 μM (40 m), and > 60 μM (30m) either during sampling or a few days prior to sampling.

766 As a result, we argue that the observed stimulation of NO<sub>2</sub><sup>-</sup> oxidation by O<sub>2</sub> (Bristow et al., 2016)  
767 occurred not because all OMZ NOB are aerobic NO<sub>2</sub><sup>-</sup> oxidizers, but instead because the location,  
768 season, and levels of O<sub>2</sub> of the sampled station selected for aerobic NOB in the source water for  
769 the purged incubations. Thus, as suggested by (Sun et al., 2017, 2021a), different NOB  
770 populations with different historical exposures to O<sub>2</sub> and adaptations likely respond differently to  
771 O<sub>2</sub> manipulations.

772 Here we built on the above previous tests of anaerobic NO<sub>2</sub><sup>-</sup> oxidation by conducting a  
773 series of incubations across an O<sub>2</sub> gradient from  $\approx$ 1 nM to 10 μM. Site waters for these  
774 incubations were drawn from the ODZ top at each SR1805 station (Table S4). We did not  
775 observe a clear inhibitory or stimulatory response of NO<sub>2</sub><sup>-</sup> oxidation to O<sub>2</sub> within the SR1805 or  
776 FK180624 stations; however, this lack of a clear response is in itself a revealing result - a lack of  
777 consistent stimulation by O<sub>2</sub> implies at least some anaerobic NOB were present. In addition, we  
778 consistently observed significant NO<sub>2</sub><sup>-</sup> oxidation at all putative O<sub>2</sub> concentrations, including 1  
779 nM, ~~a concentration usually considered functionally anoxic, a functionally anoxic oxygen~~  
780 ~~concentration, i.e., one unable to support aerobic metabolisms (Berg et al., 2022).~~ Since the  
781 ~~initial~~ O<sub>2</sub> ~~in the incubations~~ was continuously supplied by a mass flow controller and

782 subsequently checked via ~~a very sensitive~~ extremely sensitive O<sub>2</sub> sensor for all incubations,  
783 these results provide additional evidence that truly anaerobic NO<sub>2</sub><sup>-</sup> oxidation can occur.

784 One argument against our characterization of the NO<sub>2</sub><sup>-</sup> oxidation observed at ~1 nM O<sub>2</sub>  
785 as functionally anoxic is that the K<sub>m</sub> of NO<sub>2</sub><sup>-</sup> oxidation has been calculated to be as low as 0.5  
786 nM (Bristow et al., 2016). However, the data used to calculate this value have the same  
787 qualifications discussed previously: (1) the study site is at a location only anoxic during the  
788 austral summer, (2) the cruise was conducted during a time when O<sub>2</sub> intrusions would be more  
789 likely, and (3) the sampled waters experienced O<sub>2</sub> concentrations as high as 60 μM prior to  
790 sampling. Such conditions would favor aerobic NOB and the expression of high affinity NO<sub>2</sub><sup>-</sup>  
791 oxidation enzymes by these organisms when exposed to low O<sub>2</sub> conditions in incubations. As a  
792 result, we argue that the modeled K<sub>m</sub> value of 0.5 nM only applies when NOB with higher O<sub>2</sub>  
793 niches are placed in sub-micromolar O<sub>2</sub> conditions. This value does not apply to NOB observed  
794 to prefer ODZ conditions (Sun et al., 2019), which we assume would be favored under our 1 nM  
795 treatment.

796 These O<sub>2</sub> manipulation experiments also provided an opportunity to investigate the  
797 response of NO<sub>3</sub><sup>-</sup> reduction to O<sub>2</sub>. The only clear intra-station pattern that emerged from these  
798 experiments was that at station PS3, NO<sub>3</sub><sup>-</sup> reduction displayed possible inhibition by O<sub>2</sub>, as  
799 would be expected. Due to the ~~low numbers~~ small number of data points in our data set we did not  
800 attempt a kinetics fitting for this data. Interestingly, the disparity gap observed in depth profile  
801 experiments between the magnitudes of the NO<sub>3</sub><sup>-</sup> reduction and NO<sub>2</sub><sup>-</sup> oxidation rates was not  
802 observed in the O<sub>2</sub> manipulations across many O<sub>2</sub> concentrations at stations PS1 and PS2. At  
803 station PS3 a large disparity gap in the magnitudes of these processes as well as the highest  
804 overall NO<sub>3</sub><sup>-</sup> reduction rates were observed, as in the depth profile experiments (Fig. 4, 7). A



805 few of the FK180624 data points also exhibited  $\text{NO}_3^-$  reduction rates that were elevated far above  
806  $\text{NO}_2^-$  oxidation (Fig. S3). These results confirm the importance of  $\text{NO}_3^-$  reduction for the rapid  
807 recycling cycle as well as the source of  $\text{NO}_2^-$  for the SNM.

808

#### 809 **4.4 $\text{NO}_2^-$ dismutation**

810 In the absence of  $\text{O}_2$ ,  $\text{NO}_2^-$  oxidation would require another oxidant. Many candidate  
811 oxidants have been suggested. For example, iodate ( $\text{IO}_3^-$ ), an abundant marine species with  
812 global average marine concentrations of  $\sim 0.5 \mu\text{M}$  (Nozaki, 1997; Lam and Kuypers, 2011), has  
813 been proposed and shown to stimulate  $\text{NO}_2^-$  oxidation (Babbin et al., 2017). However, since  
814  $\text{IO}_3^-$  is usually absent within the ODZ core (Moriyasu et al., 2020), its low concentration makes  
815  $\text{IO}_3^-$  mediated anaerobic  $\text{NO}_2^-$  oxidation in that location unlikely (Babbin et al., 2020).  $\text{NO}_2^-$   
816 oxidation via  $\text{Mn}^{4+}$  or  $\text{Fe}^{3+}$  is thermodynamically feasible, but only at low pH ( $<6$ ) (Luther, 2010;  
817 Luther and Popp, 2002). This pH constraint, combined with the fact that concentrations of these  
818 ions are on the order of a few nM in OMZs (Kondo and Moffett, 2015; Vedamati et al., 2015),  
819 makes these mechanisms unrealistic for the ODZ core. Another proposed mechanism is that the  
820 observed  $\text{NO}_2^-$  oxidation is due to anammox, which if true should result in an observed  $\text{NO}_2^-$   
821 oxidation to anammox ratio of 0.16 – 0.3 (Kuenen, 2008; Strous et al., 1998; Oshiki et al., 2016).  
822 Instead, the observed ratio is sometimes more than 10x this range and  $\text{NO}_2^-$  oxidation is rarely  
823 observed to be less than anammox (Kalvelage et al., 2013; Babbin et al., 2020; Sun et al., 2021a).

824 Another alternative hypothesis is based on the reversibility of the nitrite oxidoreductase  
825 (NXR) enzyme. Since this enzyme has been suggested to both oxidize  $\text{NO}_2^-$  and reduce  $\text{NO}_3^-$   
826 (Kemeny et al., 2016; Koch et al., 2015; Wunderlich et al., 2013),  $\text{NO}_3^-$  reduction by NXR could  
827 over time enrich the  $^{15}\text{N}$ - $\text{NO}_3^-$  pool since lighter  $^{14}\text{NO}_3^-$  would be favored (Casciotti, 2009).

828 Even in  $^{15}\text{NO}_2^-$  tracer experiments, in which the  $\text{NO}_2^-$  pool is highly labeled, this reversibility at  
829 the enzyme site could lead to an apparent transfer of  $^{15}\text{N}$  from the  $\text{NO}_2^-$  to the  $\text{NO}_3^-$  pool if NXR  
830 mediated  $\text{NO}_3^-$  reduction was occurring. This hypothesis is supported by observations of  $\text{NO}_3^-$   
831 reduction under low  $\text{O}_2$  in cultures from the NOB genera *Nitrobacter* (Freitag et al., 1987; Bock  
832 et al., 1990), *Nitrospira* (Koch et al., 2015), and in pure cultures of *Nitrococcus mobilis* (Füssel  
833 et al., 2017). In addition, a recent study presented natural abundance isotopic evidence in pure  
834 *Nitrococcus mobilis* cultures consistent with this mechanism (Buchwald and Wankel, 2022).

835 However, NXR reversibility has not been demonstrated for the abundant (Füssel et al.,  
836 2011; Mincer et al., 2007) and sometimes predominant (Beman et al., 2013) OMZ NOB genera  
837 *Nitrospina*. Furthermore, the sole source of the isotopic evidence for the enzyme reversibility  
838 hypothesis, *Nitrococcus mobilis*, has a cytoplasm facing NXR substrate binding domain  
839 (Buchwald and Wankel, 2022), a feature found to have an established evolutionary relationship  
840 to NAR (the known  $\text{NO}_3^-$  reductase enzyme family) in other *Nitrobacter* studies (Starkenbourg et  
841 al., 2008; Kirstein and Bock, 1993). The NXR substrate binding domains in *Nitrospina* are  
842 oriented towards the periplasm and are not evolutionarily related to enzymes for  $\text{NO}_3^-$  reduction  
843 (Buchwald and Wankel, 2022; Sun et al., 2019). Due to these structural and phylogenetic  
844 differences among NOB NXR, it is possible that the *Nitrospina* NXR may be unable to perform  
845  $\text{NO}_3^-$  reduction as easily as other NOB genera. For all these reasons, it is not yet clear if the  
846 enzyme reversibility hypothesis can explain all  $\text{NO}_2^-$  oxidation measured under low  $\text{O}_2$   
847 conditions and other hypotheses should continue to be explored.

848 As a result of the above proposals' shortcomings, this paper focused on the remaining,  
849 most plausible hypothesis:  $\text{NO}_2^-$  dismutation. Our tests for dismutation rested on three  
850 hypotheses: (1) that  $\text{NO}_3^-$  additions would inhibit both  $\text{NO}_2^-$  oxidation and  $^{30}\text{N}_2$  production by

851 LeChatelier's principle, (2) that increasing  $^{15}\text{NO}_2^-$  should energetically favor dismutation,  
852 especially in treatments with no additional  $\text{NO}_3^-$ , and (3) that the ratio of non-anammox  
853 mediated  $\text{NO}_2^-$  oxidation to denitrification ( $^{30}\text{N}_2$  production) should be close to 3:1 if  $\text{NO}_2^-$   
854 dismutation explains most of the observed  $\text{NO}_2^-$  oxidation. We observed repeated inhibition of  
855  $\text{NO}_2^-$  oxidation by  $\text{NO}_3^-$  but no inhibition of  $^{30}\text{N}_2$  production due to the fact that denitrification  
856 was consistently low and insignificantly different from zero across all treatments. In treatments  
857 with 0  $\mu\text{M}$  added  $\text{NO}_3^-$ , increasing  $\text{NO}_2^-$  generally increased  $\text{NO}_2^-$  oxidation, but not  
858 denitrification. In addition, the ratio of anammox corrected  $\text{NO}_2^-$  oxidation to observed  
859 denitrification deviated from dismutation's 3:1 stoichiometry in almost all treatments. However,  
860 we did observe simultaneous inhibition of  $\text{N}_2$  and  $\text{NO}_3^-$  production as well as good agreement  
861 between the anammox corrected  $\text{NO}_2^-$  oxidation / denitrification ratio to the  $\text{NO}_2^-$  dismutation  
862 stoichiometry in one treatment - the treatment most similar to in situ conditions (60m, 0.75  $\mu\text{M}$   
863  $^{15}\text{NO}_2^-$ , 0  $\mu\text{M}$   $\text{NO}_3^-$ ). As a result, while our results show little evidence for dismutation overall,  
864 we recommend additional experiments at tracer levels similar to 0.75  $\mu\text{M}$   $^{15}\text{NO}_2^-$  to further test  
865 for  $\text{NO}_2^-$  dismutation.

866

## 867 **4.5 Relative balance of anammox and denitrification**

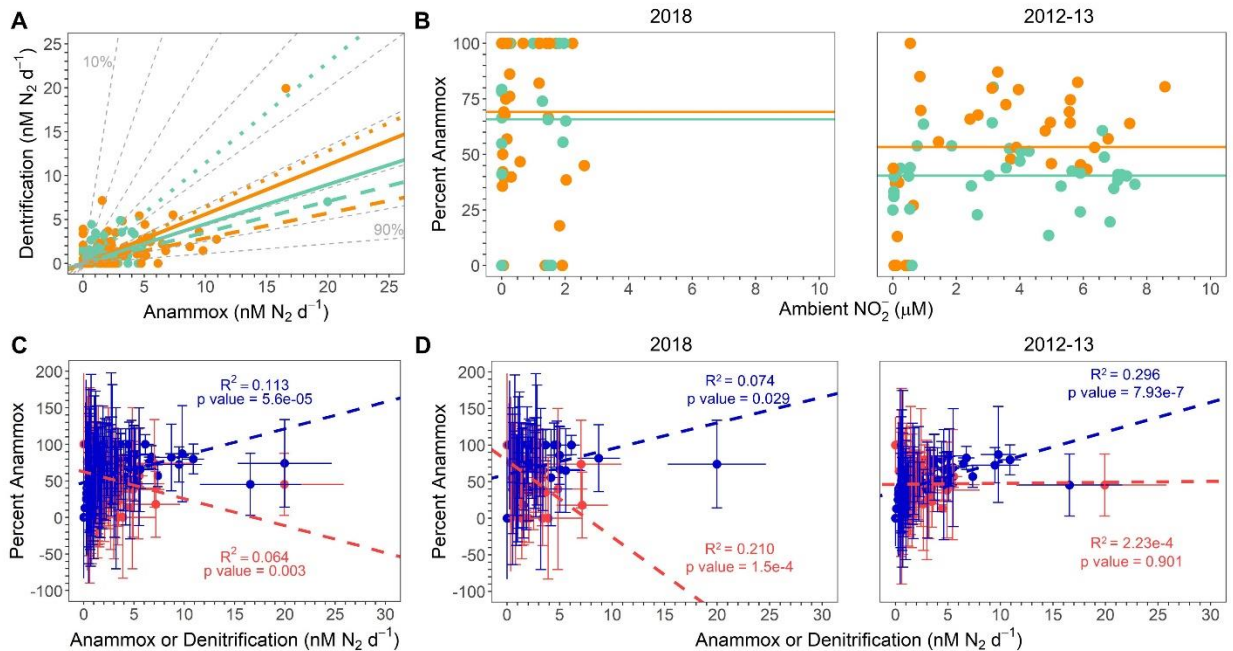
### 868 **4.5.1 Are results consistent with past observations of slow, low, and steady anammox** 869 **elevated above the predicted maximum of 29% of total N loss?**

870 According to predictions based on the composition of average marine OM (Dalsgaard et  
871 al., 2003, 2012) anammox should account for at most 29% of the total N loss flux in OMZ  
872 regions. To test this hypothesis under a variety of conditions, regressions of denitrification vs.  
873 anammox rates were calculated for all samples from the SR1805, FK180624, TN278, and

874 NBP1305 cruises. In order to compare our new data to a previous study (Babbin et al., 2020),  
875 which observed variations in the ratio of anammox and denitrification between samples from the  
876 ODZ top or above ( $\sigma_\theta < 26.4$ , “shallow boundary waters,” (Babbin et al., 2020)) and samples  
877 from the deoxygenated ODZ core or below ( $\sigma_\theta > 26.4$ , “ODZ core,” (Babbin et al., 2020)),  
878 regressions for all data (ODZ core), all data (shallow boundary), 2018 only (ODZ core), 2018  
879 only (shallow boundary), 2012-13 (TN278, and NBP1305) only (ODZ core), and 2012-13 only  
880 (shallow boundary) were calculated (Table S64). All regressions deviated from the predicted  
881 29% maximum anammox contour, although the regression from the 2012-13 cruises’ ODZ core  
882 samples was closest to the 30% anammox contour (Fig. 9A). We observed large differences in  
883 the percent anammox contours near 2012-13 and 2018 regressions. ODZ core samples from  
884 2012-13 regressed onto a line between the 40 and 50% anammox contours while ODZ core  
885 samples from 2018 regressed onto a line between the 70% and 80% anammox contours.  
886 Differences in contouring were smaller for the shallow boundary samples, although the 2018  
887 samples still regressed to a higher contour (just under 80%) than the 2013-13 samples (60%)  
888 (Fig. 9A). Our observations that all year and density based regressions fell within contours well  
889 above the theoretical prediction (Fig. 9A) and that anammox accounted for as much as 100% of  
890 the total N loss at many depths in 2018 samples (Fig. 2, Fig. 9B) is consistent with the many  
891 previous studies that observed anammox as the predominant OMZ N loss pathway (Lam et al.,  
892 2009; Thamdrup et al., 2006; Kuypers et al., 2005; Hamersley et al., 2007; Jensen et al., 2011).

893 Our new 2018 results do not contradict the idea (Dalsgaard et al., 2012) that anammox is  
894 often measured to be the bulk of total N loss but that large, episodic occurrences of denitrification  
895 can dwarf the consistent albeit low anammox contribution to total N loss. Under this view, these  
896 eruptions in denitrification return the *time integrated* balance of anammox and denitrification to

897 its expected 29 and 71% values. In this scenario, our cruises' sampling, like many but not all  
 898 others, did not coincide with episodic high rates of denitrification.



899  
 900 **Figure 9:** (A) All 2012, 2013, and 2018 denitrification and anammox rates ( $\text{nM N}_2 \text{d}^{-1}$ ), color-  
 901 coded by  $\sigma_\theta$ . ODZ core samples and lines are teal ( $\sigma_\theta > 26.4$ ) while shallow boundary samples  
 902 and lines are orange ( $\sigma_\theta < 26.4$ ). Solid, dashed, and dotted lines respectively show regressions  
 903 for all data, 2018 only, and 2012-13 data only. Dashed grey lines depict contours for percent  
 904 anammox values. See Supplementary Table S64 for regression statistics. (B) Percent anammox  
 905 vs. ambient  $\text{NO}_2^-$  for 2018 samples (left) and republished 2012 and 2013 samples (Babbin et al.,  
 906 2020) (right). Points are colored according to the same scheme as panel A. Lines show the  
 907 average percent anammox values in shallow boundary waters (orange) and the deoxygenated  
 908 ODZ core (teal). (C) Percent anammox vs. all anammox (blue) and all denitrification (red)  
 909 rates ( $\text{nM N}_2 \text{d}^{-1}$ ). Regression lines shown for % AMX vs. anammox and denitrification rates follow  
 910 the same color scheme as the data points. Error bars represent the standard error of the  
 911 regression. (D) Percent anammox vs. anammox (blue) and denitrification (red) rates ( $\text{nM N}_2 \text{d}^{-1}$ )  
 912 for 2018 only (left) and 2012-13 (right). Points and regression lines follow the same color  
 913 scheme as in panel C. Data shown in the 2012-13 only panel are republished (Babbin et al.,  
 914 2020).

915  
 916  
 917 **4.5.2 Do results support a connection between rapid  $\text{NO}_3^-$  reduction and elevated**  
 918 **anammox?**

919 Our 2018 results question the previously proposed view (Babbin et al., 2020) that rapid  
920  $\text{NO}_3^-$  reduction produces  $\text{NH}_4^+$  that in turn elevates anammox in oxycline and upper ODZ  
921 waters. While our data (Fig. 2) did find high rates of  $\text{NO}_3^-$  reduction in shallow boundary  
922 waters, the 2018 N loss data do not show elevated shallow boundary (as compared to ODZ core)  
923 percent anammox values as would be expected if high  $\text{NO}_3^-$  reduction were fueling elevated  
924 anammox in the oxycline and ODZ top. This difference between our 2018 data and some  
925 previous data (Babbin et al., 2020) in support of a connection between rapid  $\text{NO}_3^-$  reduction and  
926 elevated anammox in the oxycline and ODZ top can be seen through a comparison of shallow  
927 boundary ( $\sigma_\theta < 26.4$  (Babbin et al., 2020)) and ODZ core ( $\sigma_\theta > 26.4$  (Babbin et al., 2020)) percent  
928 anammox values in the 2018 SR1805 and FK180624 cruises against the 2012-13 TN278 and  
929 NBP1305 cruises (Fig. 9B). 2012-13 samples showed a clear partitioning between the ODZ core  
930 and shallow boundary waters in terms of percent anammox values. In 2012-13, as would be  
931 expected if high oxycline and ODZ top  $\text{NO}_3^-$  reduction were supplying  $\text{NH}_4^+$  to anammox,  
932 shallow boundary samples have a higher average percent anammox value than ODZ core  
933 samples (Fig. 9B). In 2018, this partitioning was not present - the difference between the  
934 average percent anammox values in ODZ core and shallow boundary samples was much smaller  
935 (Fig. 9B). Interestingly, the total number of samples found to be 100% anammox also sharply  
936 diverged between 2012-13 and 2018. In the 2012-13 samples, only one shallow boundary  
937 sample was found to be 100% anammox. In 2018, many samples from both shallow boundary  
938 waters and the ODZ core were 100% anammox (Fig. 9B, Fig. S6).

939 These observed differences in the partitioning of anammox and denitrification between  
940 shallow boundary waters and the ODZ core across different years and places do not support the  
941 view that  $\text{NH}_4^+$  from rapid  $\text{NO}_3^-$  reduction of oxycline and ODZ top OM always elevates

942 anammox rates. Instead, they suggest that other factors play an important role in setting the  
943 balance of anammox and denitrification. Interestingly,  $\text{NO}_2^-$  concentrations spanned a much  
944 narrower range in the two 2018 SR1805 and FK180624 cruises than the 2012-13 TN278 and  
945 NBP1305 cruises (Fig. 9B), a clue that the biogeochemical environment of the OMZ is subject to  
946 interannual variability. Observed differences in environmental variables like  $\text{NO}_2^-$  and percent  
947 anammox partitioning between 2012, 2013, and 2018 suggest that the partitioning of total N loss  
948 must depend on additional yet to be identified environmental or biological interactions.

949

#### 950 **4.5.3 Correlations of percent anammox values to anammox and denitrification rates -** 951 **comparison to previous literature**

952 In order to re-examine the result (Babbin et al., 2020) that enhanced fractions of  
953 anammox are correlated to greater anammox rates and not lower denitrification (Fig. 9D right),  
954 we created percent anammox vs. anammox and denitrification regressions with the 2018 SR1805  
955 and FK180624 data. In 2018, unlike in 2012-13 (Babbin et al., 2020), we observed significant  
956 relationships between percent anammox values and both the anammox and denitrification rates  
957 (Fig. 9D left). Regressions for the 2012-13 data showed that increases in % anammox values are  
958 correlated only to increases in anammox values, not decreases in denitrification (Babbin et al.,  
959 2020) (Fig. 9D right). The 2018 regressions, on the other hand, indicate that increases in %  
960 anammox are correlated with both increasing anammox and decreasing denitrification rates. The  
961 influence of this difference in the 2018 samples can be seen in regressions of % anammox  
962 against anammox and denitrification from all three cruises where a similar pattern to the 2018  
963 data is observed (Fig. 9C). As above, this indicates a clear difference in the partitioning of  
964 anammox and denitrification between the 2018 SR1805 and FK180624 ETNP cruises and the

965 2012-13 TN278 and NBP1305 cruises to the ETNP and ETSP. Despite the significance of the  
966 relationships, the low  $R^2$  values indicate that these relationships do not explain most of the  
967 variation in the anammox to denitrification ratio. As above, the causal mechanisms behind this  
968 variability remains to be elucidated.

969

#### 970 4.5.4 Caveats about measurements of anammox and denitrification rates

971 One bias of our sampling scheme for N loss rates is that we do not capture particle  
972 adhering denitrifiers. Most denitrifiers that encode the last two steps of denitrification are found  
973 on large particles (Ganesh et al., 2013, 2015; Fuchsman et al., 2017). As a result, measurements  
974 of complete denitrification from  $^{15}\text{NO}_2^-$  to  $^{30}\text{N}_2$  that do not capture large particle communities  
975 will underestimate the rate. Unfortunately, due to the hydrodynamics of the CTD rosette it is  
976 unlikely that large particles will be trapped inside the Niskin bottle. In addition, the nipple of  
977 each Niskin is above the bottom of the bottle. As a result, the large particles that are successfully  
978 sampled by the CTD sink to the bottom of the Niskin and are not transferred into the experiment  
979 (Suter et al., 2017).

980 Another~~One~~ important caveat to some of the above conclusions in section 4.5 is that the  
981 detection limits for anammox and denitrification rates are not identical. It is easier to detect  
982 anammox for a variety of reasons. For example, anammox from a  $^{15}\text{NH}_4^+$  tracer is more easily  
983 detected due to low background  $\text{NH}_4^+$  across most of the OMZ. Anammox from the  $^{15}\text{NO}_2^-$   
984 tracer is more detectible due to its reliance on incorporation of only a single  $^{15}\text{N}$  atom into the  
985  $^{29}\text{N}_2$  product. Denitrification, on the other hand, is more difficult to detect because of higher  
986 background  $\text{NO}_2^-$  concentrations and because definitive denitrification requires the rarer  
987 combination of two  $^{15}\text{NO}_2^-$  molecules (Babbin et al., 2017).



988 We suspect that our sampling bias against particle based denitrification and  
989 denitrification's higher detection limit may have played a role in our observations of  
990 denitrification rates in the 2012, 2013, and 2018 cruises where, for example, significant  
991 denitrification rates were only detected at four of the thirty depths sampled during SR1805  
992 (Supplementary Table S3). As a result, while the comparisons made above are helpful to  
993 examine differences in N biogeochemistry across years and stations, the true biogeochemical  
994 role of denitrification is likely greater than our tracer experiments suggest.

995 An additional important consideration is the possibility that anammox was stimulated by  
996 our tracer additions, which substantially enriched the  $\text{NO}_2^-$  and especially the  $\text{NH}_4^+$   
997 concentrations above their in situ values (see Table S7 for enrichment factors for these two  
998 nutrients' concentrations). As mentioned above, the differential control of anammox and  
999 denitrification by substrate concentration may affect the observed ratio of the two rates in tracer  
1000 incubations. Tracer additions above ambient nutrient levels are necessary to detect a mass  
1001 spectrometric signal but often can result in rates above true in situ levels. Data on the kinetic  
1002 responses of anammox and denitrification are scarce, yet another area where further research  
1003 would be very useful.

1004

1005

#### 1006 **4.6 Possibility of N loss via AOA and other N cycling processes**

1007 A recent paper (Kraft et al., 2022) reported that dense cultures of the ammonium  
1008 oxidizing archaea (AOA) *Nitrosopumilus maritimus* can support the  $\text{O}_2$  dependent process of  
1009  $\text{NH}_4^+$  oxidation in deoxygenated waters via NO disproportionation to  $\text{O}_2$  and  $\text{N}_2$ . This  
1010 mechanism would be a third N loss process that, if occurring in OMZs, would be measured as

1011 anammox or denitrification. In order to investigate the possible significance of this N loss  
1012 pathway in ODZ waters, we calculated the maximum possible N loss from  $\text{NH}_4^+$  oxidation – the  
1013 N loss that would result if all of the  $^{15}\text{N}\text{-NO}_2^-$  produced in our  $\text{NH}_4^+$  oxidation experiments was  
1014 converted into  $\text{N}_2$  via the proposed NO disproportionation reaction. These maximum  $\text{NH}_4^+$   
1015 oxidation derived N loss rates were a small fraction of the total N loss rates at most depths  
1016 (Supplementary Table S55). As a result, even these unrealistically high estimates of  $\text{N}_2$   
1017 production from AOA do not suggest that AOA are significant agents for fixed N loss. The  
1018 depths where this was not the case are all either oxic or upper oxycline depths where  $\text{NH}_4^+$   
1019 oxidation rates peak and do not require NO disproportionation to supply  $\text{O}_2$ , or depths where  
1020 equally low  $\text{NH}_4^+$  oxidation, anammox, and denitrification rates would allow a higher percentage  
1021 of the total N loss to be due to  $\text{NH}_4^+$  oxidation. As a result, our calculation argues that N loss  
1022 derived from  $\text{NH}_4^+$  oxidation is not a significant N loss flux in ODZs. Thus, we argue that our  
1023 conclusions regarding the relative balance of anammox and denitrification, as well as the  
1024 relationship of these two N loss processes to other parts of the N cycle, do not need to be revised  
1025 to account for N loss via NO disproportionation in AOA.

1026 We note that an additional N recycling pathway, dissimilatory nitrate/nitrite reduction to  
1027 ammonium (DNRA) can occur under low  $\text{O}_2$  conditions similar to those preferred by anammox  
1028 and denitrification. While some OMZ studies have found rates and *nrfA* abundances comparable  
1029 to anammox, denitrification, and  $\text{NH}_4^+$  oxidation rates and marker gene abundances (Lam et al.,  
1030 2009; Jensen et al., 2011), DNRA is best described as an extremely variable process. Other past  
1031 OMZ studies have often found negligible rates (De Brabandere et al., 2014; Kalvelage et al.,  
1032 2013; Füssel et al., 2011) and little genetic evidence for DNRA (Kalvelage et al., 2013;

1033 Fuchsman et al., 2017). Due to this variability we chose to focus this study on what are arguably  
1034 the most consistently relevant rates for OMZ N biogeochemistry.

1035

## 1036 **5 Conclusions**

1037 Nitrogen is an essential component of life and as a result, its availability can function as a  
1038 cap on biological productivity in many marine ecosystems. Since all the ocean is linked through  
1039 an intricate web of currents that span the globe, the N biogeochemistry of small regions can  
1040 affect the biogeochemistry of the rest of the ocean. Although OMZs account for just 0.1 - 1% of  
1041 the ocean's total volume (Lam and Kuypers, 2011; Codispoti and Richards, 1976; Naqvi, 1987;  
1042 Bange et al., 2000; Codispoti et al., 2005) they account for ~~320~~<sup>320-540</sup>% of all total marine N loss  
1043 (DeVries et al., 2013). As a result, developing an understanding of N cycling within OMZs is  
1044 critical for comprehending the total marine N budget. Here we presented measurements from the  
1045 ETNP OMZ of five microbial N cycling metabolisms, all of which have  $\text{NO}_2^-$  as a product,  
1046 reactant, or intermediate. Understanding the magnitudes of these rates is key to determining the  
1047 OMZ inventory of N species as well as an important piece of understanding the marine N  
1048 budget.

1049 Our results add to the growing evidence that the N recycling process of  $\text{NO}_3^-$  reduction is  
1050 the largest OMZ N flux followed by the recycling process of  $\text{NO}_2^-$  oxidation back to  $\text{NO}_3^-$ .  
1051 These two processes peaked in the oxycline or ODZ top and were usually much greater than the  
1052 two N loss processes of anammox and denitrification, a departure from the established view that  
1053 understanding N loss processes alone is the key to understanding OMZ biogeochemistry. We  
1054 also add further evidence to the body of literature that supports the occurrence of anaerobic  $\text{NO}_2^-$   
1055 oxidation in OMZ regions, most strikingly through a series of  $\text{O}_2$  manipulation experiments that

1056 show  $\text{NO}_2^-$  oxidation at putative  $\text{O}_2$  concentrations as low as 1 nM, ~~an  $\text{O}_2$  concentration so low~~  
1057 ~~that the experimental conditions are functionally anoxic.~~ We conducted experiments on waters  
1058 from two deoxygenated depths to evaluate if  $\text{NO}_2^-$  dismutation provides the oxidative power for  
1059 observed anaerobic  $\text{NO}_2^-$  oxidation and found no evidence of  $\text{NO}_2^-$  dismutation except in one  
1060 treatment – the closest to in situ  $\text{NO}_2^-$  conditions. Further exploration of the dismutation  
1061 hypothesis might therefore usefully focus on conditions near in situ  $\text{NO}_2^-$  concentrations. Across  
1062 our experiments, the percent of N loss due to anammox was consistently above the theoretical  
1063 prediction of at most 29% anammox. Our observations that  $\text{NO}_3^-$  reduction and  $\text{NO}_2^-$  oxidation  
1064 greatly surpass N loss, especially in shallow boundary waters, further reinforce the view that  
1065  $\text{NO}_2^-$  in the SNM is sourced from  $\text{NO}_3^-$  reduction.

1066 Together, these observations provide additional data that supports several new views of  
1067 OMZ biogeochemistry. We hope that our work inspires additional isotopic experiments,  
1068 culturing efforts, or genomic studies, especially those that seek to further test the occurrence of  
1069  $\text{NO}_2^-$  oxidation under functionally anoxic conditions and to examine alternative oxidants for this  
1070 process. ~~However, additional work is especially needed to further validate the occurrence of~~  
1071  ~~$\text{NO}_2^-$  oxidation under functionally anoxic conditions, explore alternative oxidants for this~~  
1072 ~~process,~~ In addition, we emphasize the importance of integrating our experimental results into  
1073 future OMZ N and C biogeochemical models and comprehend how OMZ biogeochemistry,  
1074 especially our results showing the predominance of  $\text{NO}_3^-$  reduction and  $\text{NO}_2^-$  oxidation over N  
1075 loss. The development of an accurate model of OMZ N cycling is essential towards forecasting  
1076 future changes in marine productivity and ecology as OMZs respond to ~~could change with~~  
1077 climate change and other anthropogenic ~~human-caused~~ environmental changes.

1078

1079

1080 **Author contributions**

1081 XS, CF and BBW designed, and CF performed, measured, and calculated the  $\text{NO}_3^-$  reduction and  
1082  $\text{NH}_4^+$  oxidation rates. BBW and JCT designed, BBW and JCT performed, and JCT measured  
1083 and calculated the anammox and denitrification depth profile experiments. BBW and XS  
1084 designed, JCT, BBW, and XS performed, XS and KD measured, and KD, EW, and JCT  
1085 calculated the  $\text{NO}_2^-$  oxidation depth profiles. TT and ARB designed, TT performed, DEM and  
1086 JCT measured, and EW and JCT calculated the anammox and denitrification profiles from the  
1087 FK180624 cruise. TT and ARB designed, and TT performed, measured, and calculated the  $\text{NO}_2^-$   
1088 oxidation  $\text{O}_2$  variation experiments. ARB and TT designed, TT performed, EW, XS, and JCT  
1089 measured, and EW and JCT calculated the dismutation experiments. SO provided critical help in  
1090 running the mass spectrometer to measure all samples except the oxygen variation experiments.  
1091 BBW performed the correlation and RDA analyses. JCT drafted the paper with inputs from all  
1092 authors.

1093

1094 **Competing Interests**

1095 The authors declare that they have no conflicts of interest.

1096

1097 **Data Availability**

1098 All data discussed in this manuscript will be archived in Zenodo upon publication.

1099

1100 **Acknowledgments**

1101 We would like to acknowledge the crew and scientists of the R/V *Sally Ride* and the R/V *Falkor*  
1102 for logistical and scientific support during our 2018 cruises. We thank Amal Jayakumar for  
1103 providing *amoA* and *nirS* gene abundances for the RDA and PCA analyses. We thank Emilio  
1104 Robledo-Garcia for assistance using the LUMOS sensor for the NO<sub>2</sub><sup>-</sup> oxidation O<sub>2</sub> gradient  
1105 experiments. We thank Matthias Spieler for supporting NO<sub>3</sub><sup>-</sup> reduction rate measurements in  
1106 Basel. We thank Patrick Boduch for his aid in reviewing graphics before submission. We also  
1107 acknowledge the Schmidt Ocean Institute which provided R/V *Falkor* ship time to ARB. We  
1108 thank the Simons Foundation and National Science Foundation for supporting ARB, TT, and  
1109 DEM on Simons Foundation grant 622065 and NSF grants OCE-2138890 and OCE-2142998 as  
1110 well as support for BBW, CF, JCT, and XS through NSF grant OCE-1657663.

1111

## 1112 **References**

1113 Anderson, J. J., Okubo, A., Robbins, A. S., and Richards, F. A.: A model for nitrate distributions  
1114 in oceanic oxygen minimum zones, *Deep Sea Res. Part A. Oceanogr. Res. Pap.*, 29, 1113–1140,  
1115 [https://doi.org/10.1016/0198-0149\(82\)90031-0](https://doi.org/10.1016/0198-0149(82)90031-0), 1982.

1116 ASTM International: *Standard Guide for Spiking into Aqueous Samples*, West Conshohocken,  
1117 PA, 2006.

1118 Babbin, A. R., Keil, R. G., Devol, A. H., and Ward, B. B.: Organic matter stoichiometry, flux,  
1119 and oxygen control nitrogen loss in the ocean, *Science (80-. )*, 344, 406–408,  
1120 <https://doi.org/10.1126/science.1248364>, 2014.

1121 Babbin, A. R., Peters, B. D., Mordy, C. W., Widner, B., Casciotti, K. L., and Ward, B. B.:  
1122 Multiple metabolisms constrain the anaerobic nitrite budget in the Eastern Tropical South  
1123 Pacific, *Global Biogeochem. Cycles*, 31, 258–271, <https://doi.org/10.1002/2016GB005407>,

1124 2017.

1125 Babbin, A. R., Buchwald, C., Morel, F. M. M., Wankel, S. D., and Ward, B. B.: Nitrite oxidation  
1126 exceeds reduction and fixed nitrogen loss in anoxic Pacific waters, *Mar. Chem.*, 224, 103814,  
1127 <https://doi.org/10.1016/J.MARCHEM.2020.103814>, 2020.

1128 Bange, H. W., Rixen, T., Johansen, A. M., Siefert, R. L., Ramesh, R., Ittekkot, V., Hoffmann, M.  
1129 R., and Andreae, M. O.: A revised nitrogen budget of the Arabian Sea, *Global Biogeochem.*  
1130 *Cycles*, 14, 1283–1297, <https://doi.org/10.1029/1999GB001228>, 2000.

1131 Beman, J. M., Leilei Shih, J., and Popp, B. N.: Nitrite oxidation in the upper water column and  
1132 oxygen minimum zone of the eastern tropical North Pacific Ocean, *ISME J.* 2013 711, 7, 2192–  
1133 2205, <https://doi.org/10.1038/ismej.2013.96>, 2013.

1134 Berg, J. S., Ahmerkamp, S., Pjevac, P., Hausmann, B., Milucka, J., and Kuypers, M. M. M.:  
1135 How low can they go? Aerobic respiration by microorganisms under apparent anoxia, *FEMS*  
1136 *Microbiol. Rev.*, 46, 1–14, <https://doi.org/10.1093/FEMSRE/FUAC006>, 2022.

1137 Bianchi, D., Babbin, A. R., and Galbraith, E. D.: Enhancement of anammox by the excretion of  
1138 diel vertical migrators, *Proc. Natl. Acad. Sci.*, 111, 15653–15658,  
1139 <https://doi.org/10.1073/PNAS.1410790111>, 2014.

1140 Bock, E., Koops, H. P., Möller, U. C., and Rudert, M.: A new facultatively nitrite oxidizing  
1141 bacterium, *Nitrobacter vulgaris* sp. nov., *Arch. Microbiol.* 1990 1532, 153, 105–110,  
1142 <https://doi.org/10.1007/BF00247805>, 1990.

1143 De Brabandere, L., Canfield, D. E., Dalsgaard, T., Friederich, G. E., Revsbech, N. P., Ulloa, O.,  
1144 and Thamdrup, B.: Vertical partitioning of nitrogen-loss processes across the oxic-anoxic  
1145 interface of an oceanic oxygen minimum zone, *Environ. Microbiol.*, 16, 3041–3054,  
1146 <https://doi.org/10.1111/1462-2920.12255>, 2014.

1147 Braman, R. S. and Hendrix, S. A.: Nanogram Nitrite and Nitrate Determination in Environmental  
1148 and Biological Materials by Vanadium(III) Reduction with Chemiluminescence Detection, *Anal.*  
1149 *Chem.*, 61, 2715–2718, 1989.

1150 Brandhorst, W.: Nitrification and Denitrification in the Eastern Tropical North Pacific, *J. du*  
1151 *Cons. Cons. Perm. Int. pour l’exploration la mer*, 25, 3–20, 1959.

1152 Bristow, L. A., Dalsgaard, T., Tiano, L., Mills, D. B., Bertagnolli, A. D., Wright, J. J., Hallam, S.  
1153 J., Ulloa, O., Canfield, D. E., Revsbech, N. P., and Thamdrup, B.: Ammonium and nitrite  
1154 oxidation at nanomolar oxygen concentrations in oxygen minimum zone waters, *Proc. Natl.*  
1155 *Acad. Sci. U. S. A.*, 113, 10601–10606, <https://doi.org/10.1073/PNAS.1600359113>, 2016.

1156 Bristow, L. A., Callbeck, C. M., Larsen, M., Altabet, M. A., Dekaezemacker, J., Forth, M.,  
1157 Gauns, M., Glud, R. N., Kuypers, M. M. M., Lavik, G., Milucka, J., Naqvi, S. W. A., Pratihary,  
1158 A., Revsbech, N. P., Thamdrup, B., Treusch, A. H., and Canfield, D. E.: N<sub>2</sub> production rates  
1159 limited by nitrite availability in the Bay of Bengal oxygen minimum zone, *Nat. Geosci.*, 10, 24–  
1160 29, <https://doi.org/10.1038/ngeo2847>, 2017.

1161 Buchwald, C. and Wankel, S. D.: Enzyme-catalyzed isotope equilibrium: A hypothesis to  
1162 explain apparent N cycling phenomena in low oxygen environments, *Mar. Chem.*, 244, 104140,  
1163 <https://doi.org/10.1016/J.MARCHEM.2022.104140>, 2022.

1164 Buchwald, C., Santoro, A. E., Stanley, R. H. R., and Casciotti, K. L.: Nitrogen cycling in the  
1165 secondary nitrite maximum of the eastern tropical North Pacific off Costa Rica, *Global*  
1166 *Biogeochem. Cycles*, 29, 2061–2081, <https://doi.org/10.1002/2015GB005187>, 2015.

1167 Bulow, S. E., Rich, J. J., Naik, H. S., Pratihary, A. K., and Ward, B. B.: Denitrification exceeds  
1168 anammox as a nitrogen loss pathway in the Arabian Sea oxygen minimum zone, *Deep Sea Res.*  
1169 *Part I Oceanogr. Res. Pap.*, 57, 384–393, <https://doi.org/10.1016/J.DSR.2009.10.014>, 2010.



1170 Busecke, J. J. M., Resplandy, L., Ditkovsky, S. J., and John, J. G.: Diverging Fates of the Pacific  
1171 Ocean Oxygen Minimum Zone and Its Core in a Warming World, *AGU Adv.*, 3,  
1172 e2021AV000470, <https://doi.org/10.1029/2021AV000470>, 2022.

1173 Casciotti, K. L.: Inverse kinetic isotope fractionation during bacterial nitrite oxidation, *Geochim.*  
1174 *Cosmochim. Acta*, 73, 2061–2076, <https://doi.org/10.1016/J.GCA.2008.12.022>, 2009.

1175 Casciotti, K. L., Buchwald, C., and McIlvin, M.: Implications of nitrate and nitrite isotopic  
1176 measurements for the mechanisms of nitrogen cycling in the Peru oxygen deficient zone, *Deep*  
1177 *Sea Res. Part I Oceanogr. Res. Pap.*, 80, 78–93, <https://doi.org/10.1016/J.DSR.2013.05.017>,  
1178 2013.

1179 Codispoti, L. A. and Packard, T. T.: Denitrification rates in the eastern tropical South Pacific, *J.*  
1180 *Mar. Res.*, 38, 453–477, 1980.

1181 Codispoti, L. A. and Richards, F. A.: An analysis of the horizontal regime of denitrification in  
1182 the eastern tropical North Pacific, *Limnol. Oceanogr.*, 21, 379–388,  
1183 <https://doi.org/10.4319/LO.1976.21.3.0379>, 1976.

1184 Codispoti, L. A., Brandes, J. A., Christensen, J. P., Devol, A. H., Naqvi, S. W. A., Paerl, H. W.,  
1185 and Yoshinari, T.: The oceanic fixed nitrogen and nitrous oxide budgets: Moving targets as we  
1186 enter the anthropocene?, *Sci. Mar.*, 65, 85–105, <https://doi.org/10.3989/SCIMAR.2001.65S285>,  
1187 2001.

1188 Codispoti, L. A., Yoshinari, T., and Devol, A. H.: Suboxic respiration in the oceanic water  
1189 column, in: *Respiration in Aquatic Ecosystems*, edited by: del Giorgio, P. A. and Williams, P. J.  
1190 L., Oxford University Press, 225–247, 2005.

1191 Cram, J. A., Fuchsman, C. A., Duffy, M. E., Pretty, J. L., Lekanoff, R. M., Neibauer, J. A.,  
1192 Leung, S. W., Huebert, K. B., Weber, T. S., Bianchi, D., Evans, N., Devol, A. H., Keil, R. G.,

1193 and McDonnell, A. M. P.: Slow Particle Remineralization, Rather Than Suppressed  
1194 Disaggregation, Drives Efficient Flux Transfer Through the Eastern Tropical North Pacific  
1195 Oxygen Deficient Zone, *Global Biogeochem. Cycles*, 36, e2021GB007080,  
1196 <https://doi.org/10.1029/2021GB007080>, 2022.

1197 Dalsgaard, T., Canfield, D. E., Peterson, J., Thamdrup, B., and Acuna-Gonzales, J.: N production  
1198 by anamox in the anoxic water column of Golfo Dulce, Costa Rica., *Nature*, 422, 606–608,  
1199 <https://doi.org/10.1038/nature01526>, 2003.

1200 Dalsgaard, T., Thamdrup, B., Fariás, L., and Revsbech, N. P.: Anammox and denitrification in  
1201 the oxygen minimum zone of the eastern South Pacific, *Limnol. Oceanogr.*, 57, 1331–1346,  
1202 <https://doi.org/10.4319/lo.2012.57.5.1331>, 2012.

1203 DeVries, T., Deutsch, C., Rafter, P. A., and Primeau, F.: Marine denitrification rates determined  
1204 from a global 3-D inverse model, *Biogeosciences*, 10, 2481–2496, [https://doi.org/10.5194/BG-](https://doi.org/10.5194/BG-10-2481-2013)  
1205 10-2481-2013, 2013.

1206 Freitag, A., Rudert, M., and Bock, E.: Growth of *Nitrobacter* by dissimilatory nitrate reduction,  
1207 *FEMS Microbiol. Lett.*, 48, 105–109, <https://doi.org/10.1111/J.1574-6968.1987.TB02524.X>,  
1208 1987.

1209 Frey, C., Bange, H. W., Achterberg, E. P., Jayakumar, A., Löscher, C. R., Arévalo-Martínez, D.  
1210 L., León-Palmero, E., Sun, M., Sun, X., Xie, R. C., Oleynik, S., and Ward, B. B.: Regulation of  
1211 nitrous oxide production in low-oxygen waters off the coast of Peru, *Biogeosciences*, 17, 2263–  
1212 2287, <https://doi.org/10.5194/BG-17-2263-2020>, 2020.

1213 Frey, C., Sun, X., Szemberski, L., Casciotti, K. L., Garcia-Robledo, E., Jayakumar, A., Kelly, C.  
1214 L., and Lehmann, M. F.: Nitrous oxide production kinetics from ammonia oxidation in the  
1215 Eastern Tropical North Pacific, *Limnol. Oceanogr.*, Under review, 2022.

1216 Fuchsman, C. A., Devol, A. H., Saunders, J. K., McKay, C., and Rocap, G.: Niche partitioning of  
1217 the N cycling microbial community of an offshore oxygen deficient zone, *Front. Microbiol.*, 8,  
1218 2384, <https://doi.org/10.3389/FMICB.2017.02384/BIBTEX>, 2017.

1219 Fuchsman, C. A., Palevsky, H. I., Widner, B., Duffy, M., Carlson, M. C. G., Neibauer, J. A.,  
1220 Mulholland, M. R., Keil, R. G., Devol, A. H., and Rocap, G.: Cyanobacteria and cyanophage  
1221 contributions to carbon and nitrogen cycling in an oligotrophic oxygen-deficient zone, *ISME J.*  
1222 2019 1311, 13, 2714–2726, <https://doi.org/10.1038/s41396-019-0452-6>, 2019.

1223 Füssel, J., Lam, P., Lavik, G., Jensen, M. M., Holtappels, M., Günter, M., and Kuypers, M. M.  
1224 M.: Nitrite oxidation in the Namibian oxygen minimum zone, *ISME J.*, 6, 1200–1209,  
1225 <https://doi.org/10.1038/ismej.2011.178>, 2011.

1226 Füssel, J., Lückner, S., Yilmaz, P., Nowka, B., van Kessel, M. A. H. J., Bourceau, P., Hach, P. F.,  
1227 Littmann, S., Berg, J., Spieck, E., Daims, H., Kuypers, M. M. M., and Lam, P.: Adaptability as  
1228 the key to success for the ubiquitous marine nitrite oxidizer *Nitrococcus*, *Sci. Adv.*, 3,  
1229 [https://doi.org/10.1126/SCIADV.1700807/SUPPL\\_FILE/1700807\\_TABLES1\\_TO\\_S10.ZIP](https://doi.org/10.1126/SCIADV.1700807/SUPPL_FILE/1700807_TABLES1_TO_S10.ZIP),  
1230 2017.

1231 Ganesh, S., Parris, D. J., Delong, E. F., and Stewart, F. J.: Metagenomic analysis of size-  
1232 fractionated picoplankton in a marine oxygen minimum zone, *ISME J.* 2014 81, 8, 187–211,  
1233 <https://doi.org/10.1038/ismej.2013.144>, 2013.

1234 Ganesh, S., Bristow, L. A., Larsen, M., Sarode, N., Thamdrup, B., and Stewart, F. J.: Size-  
1235 fraction partitioning of community gene transcription and nitrogen metabolism in a marine  
1236 oxygen minimum zone, *ISME J.* 2015 912, 9, 2682–2696, <https://doi.org/10.1038/ismej.2015.44>,  
1237 2015.

1238 Garcia-Robledo, E., Borisov, S., Klimant, I., and Revsbech, N. P.: Determination of respiration

1239 rates in water with sub-micromolar oxygen concentrations, *Front. Mar. Sci.*, 3, 244,  
1240 <https://doi.org/10.3389/FMARS.2016.00244/BIBTEX>, 2016.

1241 Garcia-Robledo, E., Padilla, C. C., Aldunate, M., Stewart, F. J., Ulloa, O., Paulmier, A., Gregori,  
1242 G., and Revsbech, N. P.: Cryptic oxygen cycling in anoxic marine zones, *Proc. Natl. Acad. Sci.*  
1243 U. S. A., 114, 8319–8324, <https://doi.org/10.1073/PNAS.1619844114>, 2017.

1244 Garcia-Robledo, E., Paulmier, A., Borisov, S. M., and Revsbech, N. P.: Sampling in low oxygen  
1245 aquatic environments: The deviation from anoxic conditions, *Limnol. Oceanogr. Methods*, 19,  
1246 733–740, <https://doi.org/10.1002/LOM3.10457>, 2021.

1247 Granger, J., & Sigman, D. M.: Removal of nitrite with sulfamic acid for nitrate N and O isotope  
1248 analysis with the denitrifier method, *Rapid Commun. Mass Spectrom.*, 23, 3753–3762., *Rapid*  
1249 *Commun. Mass Spectrom.*, 23, 3753–3762, <https://doi.org/10.1002/rcm>, 2009.

1250 Granger, J. and Wankel, S. D.: Isotopic overprinting of nitrification on denitrification as a  
1251 ubiquitous and unifying feature of environmental nitrogen cycling, *Proc. Natl. Acad. Sci. U. S.*  
1252 *A.*, 113, E6391–E6400,  
1253 [https://doi.org/10.1073/PNAS.1601383113/SUPPL\\_FILE/PNAS.201601383SI.PDF](https://doi.org/10.1073/PNAS.1601383113/SUPPL_FILE/PNAS.201601383SI.PDF), 2016.

1254 Hamersley, M. R., Lavik, G., Woebken, D., Rattray, J. E., Lam, P., Hopmans, E. C., Sinninghe  
1255 Damsté, J. S., Krüger, S., Graco, M., Gutiérrez, D., and Kuypers, M. M. M.: Anaerobic  
1256 ammonium oxidation in the Peruvian oxygen minimum zone, *Limnol. Oceanogr.*, 52, 923–933,  
1257 <https://doi.org/10.4319/LO.2007.52.3.0923>, 2007.

1258 Holmes, R. M., Aminot, A., Kérouel, R., Hooker, B. A., and Peterson, B. J.: A simple and  
1259 precise method for measuring ammonium in marine and freshwater ecosystems, *Can. J. Fish.*  
1260 *Aquat. Sci.*, 56, 1801–1808, <https://doi.org/10.1139/f99-128>, 1999.

1261 Horak, R. E. A., Ruef, W., Ward, B. B., and Devol, A. H.: Expansion of denitrification and

1262 anoxia in the eastern tropical North Pacific from 1972 to 2012, *Geophys. Res. Lett.*, 43, 5252–  
1263 5260, <https://doi.org/10.1002/2016GL068871>, 2016.

1264 Ito, T., Minobe, S., Long, M. C., and Deutsch, C.: Upper ocean O<sub>2</sub> trends: 1958–2015, *Geophys.*  
1265 *Res. Lett.*, 44, 4214–4223, <https://doi.org/10.1002/2017GL073613>, 2017.

1266 Jayakumar, A., Wajih, S., Naqvi, A., and Ward, B. B.: Distribution and Relative Quantification  
1267 of Key Genes Involved in Fixed Nitrogen Loss From the Arabian Sea Oxygen Minimum Zone,  
1268 *Indian Ocean Biogeochem. Process. Ecol. Var. Geophys. Monogr. Ser.*, 185,  
1269 <https://doi.org/10.1029/2008GM000730>, 2009.

1270 Jensen, M. M., Lam, P., Revsbech, N. P., Nagel, B., Gaye, B., Jetten, M. S. M., and Kuypers, M.  
1271 M. M.: Intensive nitrogen loss over the Omani Shelf due to anammox coupled with dissimilatory  
1272 nitrite reduction to ammonium, *ISME J.* 2011 510, 5, 1660–1670,  
1273 <https://doi.org/10.1038/ismej.2011.44>, 2011.

1274 Kalvelage, T., Lavik, G., Lam, P., Contreras, S., Arteaga, L., Löscher, C. R., Oschlies, A.,  
1275 Paulmier, A., Stramma, L., and M Kuypers, M. M.: Nitrogen cycling driven by organic matter  
1276 export in the South Pacific oxygen minimum zone, 55812, <https://doi.org/10.1038/NGEO1739>,  
1277 2013.

1278 Keeling, R. F., Körtzinger, A., and Gruber, N.: Ocean deoxygenation in a warming world, *Ann.*  
1279 *Rev. Mar. Sci.*, 2, 199–229, <https://doi.org/10.1146/annurev.marine.010908.163855>, 2010.

1280 Kemeny, P. C., Weigand, M. A., Zhang, R., Carter, B. R., Karsh, K. L., Fawcett, S. E., and  
1281 Sigman, D. M.: Enzyme-level interconversion of nitrate and nitrite in the fall mixed layer of the  
1282 Antarctic Ocean, *Global Biogeochem. Cycles*, 30, 1069–1085,  
1283 <https://doi.org/10.1002/2015GB005350>, 2016.

1284 Kirstein, K. and Bock, E.: Close genetic relationship between *Nitrobacter hamburgensis* nitrite

1285 oxidoreductase and Escherichia coli nitrate reductases, Arch. Microbiol. 1993 1606, 160, 447–  
1286 453, <https://doi.org/10.1007/BF00245305>, 1993.

1287 Koch, H., Lücker, S., Albertsen, M., Kitzinger, K., Herbold, C., Spieck, E., Nielsen, P. H.,  
1288 Wagner, M., and Daims, H.: Expanded metabolic versatility of ubiquitous nitrite-oxidizing  
1289 bacteria from the genus Nitrospira, Proc. Natl. Acad. Sci. U. S. A., 112, 11371–11376,  
1290 <https://doi.org/10.1073/PNAS.1506533112>, 2015.

1291 Kondo, Y. and Moffett, J. W.: Iron redox cycling and subsurface offshore transport in the eastern  
1292 tropical South Pacific oxygen minimum zone, Mar. Chem., 168, 95–103,  
1293 <https://doi.org/10.1016/J.MARCHEM.2014.11.007>, 2015.

1294 Kraft, B., Jehmlich, N., Larsen, M., Bristow, L. A., Könneke, M., Thamdrup, B., and Canfield,  
1295 D. E.: Oxygen and nitrogen production by an ammonia-oxidizing archaeon, Science (80-. ), 375,  
1296 97–100,  
1297 [https://doi.org/10.1126/SCIENCE.ABE6733/SUPPL\\_FILE/SCIENCE.ABE6733\\_MDAR\\_REPR](https://doi.org/10.1126/SCIENCE.ABE6733/SUPPL_FILE/SCIENCE.ABE6733_MDAR_REPR)  
1298 ODOCIBILITY\_CHECKLIST.PDF, 2022.

1299 Kuenen, J. G.: Anammox bacteria from discovery, 6, <https://doi.org/10.1038/nrmicro1857>, 2008.

1300 Kuypers, M. M. M., Lavik, G., Woebken, D., Schmid, M., Fuchs, B. M., Amann, R., Jørgensen,  
1301 B. B., and Jetten, M. S. M.: Massive nitrogen loss from the Benguela upwelling system through  
1302 anaerobic ammonium oxidation, Proc. Natl. Acad. Sci. U. S. A., 102, 6478–6483,  
1303 <https://doi.org/10.1073/PNAS.0502088102>, 2005.

1304 Lam, P. and Kuypers, M. M. M.: Microbial Nitrogen Cycling Processes in Oxygen Minimum  
1305 Zones, Ann. Rev. Mar. Sci., 3, 317–345, <https://doi.org/10.1146/annurev-marine-120709->  
1306 142814, 2011.

1307 Lam, P., Lavik, G., Jensen, M. M., Van Vossenberg, J. De, Schmid, M., Woebken, D., Gutiérrez,

1308 D., Amann, R., Jetten, M. S. M., and Kuypers, M. M. M.: Revising the nitrogen cycle in the  
1309 Peruvian oxygen minimum zone, *Proc. Natl. Acad. Sci. U. S. A.*, 106, 4752–4757,  
1310 <https://doi.org/10.1073/PNAS.0812444106>, 2009.

1311 Lam, P., Jensen, M. M., Kock, A., Lettmann, K. A., Plancherel, Y., Lavik, G., Bange, H. W., and  
1312 Kuypers, M. M. M.: Origin and fate of the secondary nitrite maximum in the Arabian Sea,  
1313 *Biogeosciences*, 8, 1565–1577, <https://doi.org/10.5194/BG-8-1565-2011>, 2011.

1314 Van de Leemput, I. A., Veraart, A. J., Dakos, V., De Klein, J. J. M., Strous, M., and Scheffer,  
1315 M.: Predicting microbial nitrogen pathways from basic principles, *Environ. Microbiol.*, 13,  
1316 1477–1487, <https://doi.org/10.1111/J.1462-2920.2011.02450.X>, 2011.

1317 Lehner, P., Larndorfer, C., Garcia-Robledo, E., Larsen, M., Borisov, S. M., Revsbech, N. P.,  
1318 Glud, R. N., Canfield, D. E., and Klimant, I.: LUMOS - A Sensitive and Reliable Optode System  
1319 for Measuring Dissolved Oxygen in the Nanomolar Range, *PLoS One*, 10, e0128125,  
1320 <https://doi.org/10.1371/JOURNAL.PONE.0128125>, 2015.

1321 Lipschultz, F., Wofsy, S. C., Ward, B. B., Codispoti, L. A., Friedrich, G., and Elkins, J. W.:  
1322 Bacterial transformations of inorganic nitrogen in the oxygen-deficient waters of the Eastern  
1323 Tropical South Pacific Ocean, *Deep Sea Res. Part A. Oceanogr. Res. Pap.*, 37, 1513–1541,  
1324 [https://doi.org/10.1016/0198-0149\(90\)90060-9](https://doi.org/10.1016/0198-0149(90)90060-9), 1990.

1325 Lomas, M. W. and Lipschultz, F.: Forming the primary nitrite maximum: Nitrifiers or  
1326 phytoplankton?, *Limnol. Oceanogr.*, 51, 2453–2467, <https://doi.org/10.4319/LO.2006.51.5.2453>,  
1327 2006.

1328 Luther, G. W.: The role of one- and two-electron transfer reactions in forming  
1329 thermodynamically unstable intermediates as barriers in multi-electron redox reactions, *Aquat.*  
1330 *Geochemistry*, 16, 395–420, <https://doi.org/10.1007/S10498-009-9082-3/FIGURES/14>, 2010.

1331 Luther, G. W. and Popp, J. I.: Kinetics of the Abiotic Reduction of Polymeric Manganese  
1332 Dioxide by Nitrite: An Anaerobic Nitrification Reaction, *Aquat. Geochemistry* 2002 81, 8, 15–  
1333 36, <https://doi.org/10.1023/A:1020325604920>, 2002.

1334 Margolskee, A., Frenzel, H., Emerson, S., and Deutsch, C.: Ventilation Pathways for the North  
1335 Pacific Oxygen Deficient Zone, *Global Biogeochem. Cycles*, 33, 875–890,  
1336 <https://doi.org/10.1029/2018GB006149>, 2019.

1337 Martin, J. H., Knauer, G. A., Karl, D. M., and Broenkow, W. W.: VERTEX: carbon cycling in  
1338 the northeast Pacific, *Deep Sea Res. Part A. Oceanogr. Res. Pap.*, 34, 267–285,  
1339 [https://doi.org/10.1016/0198-0149\(87\)90086-0](https://doi.org/10.1016/0198-0149(87)90086-0), 1987.

1340 McIlvin, M. R. and Altabet, M. A.: Chemical conversion of nitrate and nitrite to nitrous oxide for  
1341 nitrogen and oxygen isotopic analysis in freshwater and seawater, *Anal. Chem.*, 77, 5589–5595,  
1342 <https://doi.org/10.1021/ac050528s>, 2005.

1343 Mincer, T. J., Church, M. J., Taylor, L. T., Preston, C., Karl, D. M., and DeLong, E. F.:  
1344 Quantitative distribution of presumptive archaeal and bacterial nitrifiers in Monterey Bay and the  
1345 North Pacific Subtropical Gyre, *Environ. Microbiol.*, 9, 1162–1175,  
1346 <https://doi.org/10.1111/J.1462-2920.2007.01239.X>, 2007.

1347 Monreal, P. J., Kelly, C. L., Travis, N. M., and Casciotti, K. L.: Identifying the Sources and  
1348 Drivers of Nitrous Oxide Accumulation in the Eddy-Influenced Eastern Tropical North Pacific  
1349 Oxygen-Deficient Zone, *Global Biogeochem. Cycles*, 36, e2022GB007310,  
1350 <https://doi.org/10.1029/2022GB007310>, 2022.

1351 Moriyasu, R., Evans, N., Bolster, K. M., Hardisty, D. S., and Moffett, J. W.: The Distribution  
1352 and Redox Speciation of Iodine in the Eastern Tropical North Pacific Ocean, *Global  
1353 Biogeochem. Cycles*, 34, e2019GB006302, <https://doi.org/10.1029/2019GB006302>, 2020.



1354 Naqvi, S. W. A.: Some aspects of the oxygen-deficient conditions and denitrification in the  
1355 Arabian Sea, *J. Mar. Res.*, 45, 1049–1072, 1987.

1356 Nozaki, Y.: A fresh look at element distribution in the North Pacific Ocean, *Eos, Trans. Am.*  
1357 *Geophys. Union*, 78, 221–221, <https://doi.org/10.1029/97EO00148>, 1997.

1358 Oshiki, M., Satoh, H., and Okabe, S.: Ecology and physiology of anaerobic ammonium oxidizing  
1359 bacteria, *Environ. Microbiol.*, 18, 2784–2796, [https://doi.org/10.1111/1462-](https://doi.org/10.1111/1462-2920.13134/SUPPINFO)  
1360 [2920.13134/SUPPINFO](https://doi.org/10.1111/1462-2920.13134/SUPPINFO), 2016.

1361 Padilla, C. C., Bristow, L. A., Sarode, N., Garcia-Robledo, E., Gómez Ramírez, E., Benson, C.  
1362 R., Bourbonnais, A., Altabet, M. A., Girguis, P. R., Thamdrup, B., and Stewart, F. J.: NC10  
1363 bacteria in marine oxygen minimum zones, *ISME J.* 2016 108, 10, 2067–2071,  
1364 <https://doi.org/10.1038/ismej.2015.262>, 2016.

1365 Peng, X., Fuchsman, C. A., Jayakumar, A., Oleynik, S., Martens-Habbena, W., Devol, A. H., and  
1366 Ward, B. B.: Ammonia and nitrite oxidation in the Eastern Tropical North Pacific, *Global*  
1367 *Biogeochem. Cycles*, 29, 2034–2049, <https://doi.org/10.1002/2015GB005278>, 2015.

1368 Peng, X., Fuchsman, C. A., Jayakumar, A., Warner, M. J., Devol, A. H., and Ward, B. B.:  
1369 Revisiting nitrification in the Eastern Tropical South Pacific: A focus on controls, *J. Geophys.*  
1370 *Res. Ocean.*, 121, 1667–1684, <https://doi.org/10.1002/2015JC011455>, 2016.

1371 Penn, J., Weber, T., and Deutsch, C.: Microbial functional diversity alters the structure and  
1372 sensitivity of oxygen deficient zones, *Geophys. Res. Lett.*, 43, 9773–9780,  
1373 <https://doi.org/10.1002/2016GL070438>, 2016.

1374 Peters, B. D., Babbin, A. R., Lettmann, K. A., Mordy, C. W., Ulloa, O., Ward, B. B., and  
1375 Casciotti, K. L.: Vertical modeling of the nitrogen cycle in the eastern tropical South Pacific  
1376 oxygen deficient zone using high-resolution concentration and isotope measurements, *Global*

1377 Biogeochem. Cycles, 30, 1661–1681, <https://doi.org/10.1002/2016GB005415>, 2016.

1378 R: A language and environment for statistical computing:

1379 Starkenburg, S. R., Larimer, F. W., Stein, L. Y., Klotz, M. G., Chain, P. S. G., Sayavedra-Soto,  
1380 L. A., Poret-Peterson, A. T., Gentry, M. E., Arp, D. J., Ward, B., and Bottomley, P. J.: Complete  
1381 genome sequence of *Nitrobacter hamburgensis* X14 and comparative genomic analysis of  
1382 species within the genus *Nitrobacter*, *Appl. Environ. Microbiol.*, 74, 2852–2863,  
1383 [https://doi.org/10.1128/AEM.02311-07/SUPPL\\_FILE/SUPPLEMENTAL\\_TABLE\\_2.PDF](https://doi.org/10.1128/AEM.02311-07/SUPPL_FILE/SUPPLEMENTAL_TABLE_2.PDF),  
1384 2008.

1385 Stramma, L., Johnson, G. C., Sprintall, J., and Mohrholz, V.: Expanding oxygen-minimum zones  
1386 in the tropical oceans, *Science (80-. )*, 320, 655–658,  
1387 [https://doi.org/10.1126/SCIENCE.1153847/ASSET/09F7EF41-9228-40BD-8E17-  
1388 06C4E9218CC5/ASSETS/GRAPHIC/320\\_655\\_F2.JPEG](https://doi.org/10.1126/SCIENCE.1153847/ASSET/09F7EF41-9228-40BD-8E17-06C4E9218CC5/ASSETS/GRAPHIC/320_655_F2.JPEG), 2008.

1389 Strickland, J. D. H. and Parsons, T. R.: *A Practical Handbook of Seawater Analysis*, Fisheries  
1390 Research Board of Canada, Ottawa, 1972.

1391 Strohm, T. O., Griffin, B., Zumft, W. G., and Schink, B.: Growth yields in bacterial  
1392 denitrification and nitrate ammonification, *Appl. Environ. Microbiol.*, 73, 1420–1424,  
1393 [https://doi.org/10.1128/AEM.02508-06/ASSET/88AA1997-7BB3-42B6-A761-  
1394 DCB47D972CA6/ASSETS/GRAPHIC/ZAM0050775730001.JPEG](https://doi.org/10.1128/AEM.02508-06/ASSET/88AA1997-7BB3-42B6-A761-DCB47D972CA6/ASSETS/GRAPHIC/ZAM0050775730001.JPEG), 2007.

1395 Strous, M., Heijnen, J. J., Kuenen, J. G., and Jetten, M. S. M.: The sequencing batch reactor as a  
1396 powerful tool for the study of slowly growing anaerobic ammonium-oxidizing microorganisms,  
1397 *Appl. Microbiol. Biotechnol.* 1998 505, 50, 589–596, <https://doi.org/10.1007/S002530051340>,  
1398 1998.

1399 Sun, X. and Ward, B. B.: Novel metagenome-assembled genomes involved in the nitrogen cycle

1400 from a Pacific oxygen minimum zone, *ISME Commun.* 2021 11, 1, 1–5,  
1401 <https://doi.org/10.1038/s43705-021-00030-2>, 2021.

1402 Sun, X., Ji, Q., Jayakumar, A., and Ward, B. B.: Dependence of nitrite oxidation on nitrite and  
1403 oxygen in low-oxygen seawater, *Geophys. Res. Lett.*, 44, 7883–7891,  
1404 <https://doi.org/10.1002/2017GL074355>, 2017.

1405 Sun, X., Kop, L. F. M., Lau, M. C. Y., Frank, J., Jayakumar, A., Lücker, S., and Ward, B. B.:  
1406 Uncultured Nitrospina-like species are major nitrite oxidizing bacteria in oxygen minimum  
1407 zones, *ISME J.*, <https://doi.org/10.1038/s41396-019-0443-7>, 2019.

1408 Sun, X., Frey, C., Garcia-Robledo, E., Jayakumar, A., and Ward, B. B.: Microbial niche  
1409 differentiation explains nitrite oxidation in marine oxygen minimum zones, *ISME J.* 2021 155,  
1410 15, 1317–1329, <https://doi.org/10.1038/s41396-020-00852-3>, 2021.

1411 Sun, X., Frey, C., and Ward, B. B.: Nitrite Oxidation Across the Full Oxygen Spectrum in the  
1412 Ocean, *Global Biogeochem. Cycles*, 37, e2022GB007548,  
1413 <https://doi.org/10.1029/2022GB007548>, 2023.

1414 Suter, E. A., Scranton, M. I., Chow, S., Stinton, D., Medina Faull, L., and Taylor, G. T.: Niskin  
1415 bottle sample collection aliases microbial community composition and biogeochemical  
1416 interpretation, *Limnol. Oceanogr.*, 62, 606–617, <https://doi.org/10.1002/LNO.10447>, 2017.

1417 Tang, W., Tracey, J. C., Carroll, J., Wallace, E., Lee, J. A., Nathan, L., Sun, X., Jayakumar, A.,  
1418 and Ward, B. B.: Nitrous oxide production in the Chesapeake Bay, *Limnol. Oceanogr.*, 67,  
1419 2101–2116, <https://doi.org/10.1002/LNO.12191>, 2022.

1420 Taylor, B. W., Keep, C. F., Hall, R. O., Koch, B. J., Tronstad, L. M., Flecker, A. S., and Ulseth,  
1421 A. J.: Improving the fluorometric ammonium method: matrix effects, background fluorescence,  
1422 and standard additions, *Am. Benthol. Soc.*, 26, 167–177, <https://doi.org/10.1899/0887-3593>,

1423 2007.

1424 Thamdrup, B. and Dalsgaard, T.: The fate of ammonium in anoxic manganese oxide-rich marine  
1425 sediment, *Geochim. Cosmochim. Acta*, 64, 4157–4164, [https://doi.org/10.1016-](https://doi.org/10.1016/S0016-7037(00)00496-8)  
1426 [7037\(00\)00496-8](https://doi.org/10.1016/S0016-7037(00)00496-8), 2000.

1427 Thamdrup, B. and Dalsgaard, T.: Production of N<sub>2</sub> through anaerobic ammonium oxidation  
1428 coupled to nitrate reduction in marine sediments, *Appl. Environ. Microbiol.*, 68, 1312–1318,  
1429 <https://doi.org/10.1128/AEM.68.3.1312-1318.2002>/ASSET/F1579424-64C0-464C-AF9C-  
1430 5BEB3458C869/ASSETS/GRAPHIC/AM0321630005.JPEG, 2002.

1431 Thamdrup, B., Dalsgaard, T., Jensen, M. M., Ulloa, O., Farías, L., and Escribano, R.: Anaerobic  
1432 ammonium oxidation in the oxygen-deficient waters off northern Chile, *Limnol. Oceanogr.*, 51,  
1433 2145–2156, <https://doi.org/10.4319/LO.2006.51.5.2145>, 2006.

1434 Tiano, L., Garcia-Robledo, E., Dalsgaard, T., Devol, A. H., Ward, B. B., Ulloa, O., Canfield, D.  
1435 E., and Peter Revsbech, N.: Oxygen distribution and aerobic respiration in the north and south  
1436 eastern tropical Pacific oxygen minimum zones, *Deep Sea Res. Part I Oceanogr. Res. Pap.*, 94,  
1437 173–183, <https://doi.org/10.1016/J.DSR.2014.10.001>, 2014.

1438 Tsementzi, D., Wu, J., Deutsch, S., Nath, S., Rodriguez-R, L. M., Burns, A. S., Ranjan, P.,  
1439 Sarode, N., Malmstrom, R. R., Padilla, C. C., Stone, B. K., Bristow, L. A., Larsen, M., Glass, J.  
1440 B., Thamdrup, B., Woyke, T., Konstantinidis, K. T., and Stewart, F. J.: SAR11 bacteria linked to  
1441 ocean anoxia and nitrogen loss, *Nature*, 536, 179–183, <https://doi.org/10.1038/nature19068>,  
1442 2016.

1443 Ulloa, O., Canfield, D. E., DeLong, E. F., Letelier, R. M., and Stewart, F. J.: Microbial  
1444 oceanography of anoxic oxygen minimum zones, *Proc. Natl. Acad. Sci. U. S. A.*, 109, 15996–  
1445 16003, <https://doi.org/10.1073/PNAS.1205009109>, 2012.

1446 Vedamati, J., Chan, C., and Moffett, J. W.: Distribution of dissolved manganese in the Peruvian  
1447 Upwelling and Oxygen Minimum Zone, *Geochim. Cosmochim. Acta*, 156, 222–240,  
1448 <https://doi.org/10.1016/J.GCA.2014.10.026>, 2015.

1449 Wanninkhof, R.: Relationship between wind speed and gas exchange over the ocean, *J. Geophys.*  
1450 *Res. Ocean.*, 97, 7373–7382, <https://doi.org/10.1029/92JC00188>, 1992.

1451 Ward, B. B., Glover, H. E., and Lipschultz, F.: Chemoautotrophic activity and nitrification in the  
1452 oxygen minimum zone off Peru, *Deep Sea Res. Part A. Oceanogr. Res. Pap.*, 36, 1031–1051,  
1453 [https://doi.org/10.1016/0198-0149\(89\)90076-9](https://doi.org/10.1016/0198-0149(89)90076-9), 1989.

1454 Ward, B. B., Tuit, C. B., Jayakumar, A., Rich, J. J., Moffett, J., and Naqvi, S. W. A.: Organic  
1455 carbon, and not copper, controls denitrification in oxygen minimum zones of the ocean, *Deep*  
1456 *Sea Res. Part I Oceanogr. Res. Pap.*, 55, 1672–1683, <https://doi.org/10.1016/J.DSR.2008.07.005>,  
1457 2008.

1458 Ward, B. B., Devol, A. H., Rich, J. J., Chang, B. X., Bulow, S. E., Naik, H., Pratihary, A., and  
1459 Jayakumar, A.: Denitrification as the dominant nitrogen loss process in the Arabian Sea, *Nat.*  
1460 2009 4617260, 461, 78–81, <https://doi.org/10.1038/nature08276>, 2009.

1461 Weigand, M. A., Foriel, J., Barnett, B., Oleynik, S., and Sigman, D. M.: Updates to  
1462 instrumentation and protocols for isotopic analysis of nitrate by the denitrifier method, *Rapid*  
1463 *Commun. Mass Spectrom.*, 30, 1365–1383, <https://doi.org/10.1002/rcm.7570>, 2016.

1464 Wunderlich, A., Meckenstock, R. U., and Einsiedl, F.: A mixture of nitrite-oxidizing and  
1465 denitrifying microorganisms affects the  $\delta^{18}\text{O}$  of dissolved nitrate during anaerobic microbial  
1466 denitrification depending on the  $\delta^{18}\text{O}$  of ambient water, *Geochim. Cosmochim. Acta*, 119, 31–  
1467 45, <https://doi.org/10.1016/J.GCA.2013.05.028>, 2013.

1468